**P**eople's **D**emocratic **R**epublic of **A**lgeria **M**inistry of
**H**igher **E**ducation and **S**cientific **R**esearch
University of 20 Aout1955-
Skikda
Faculty of Sciences
Department of Physics

N° : .....

# Master Thesis

**Division :** Physics

**Specialty :** Material Physics

## Thesis entitled :

**Elaboration of binary semiconductors with spray method for optoelectronics applications**

**Presented by:**
Hadjoudja Ghofrane

Soutenu le: 01 /07 /2025 devant le jury composé de:

| | | | |
|---|---|---|---|
| Boulkhessaim Salim | MCA | University of Skikda | President |
| Kamli Kenza | MCA | University of Skikda | Rapporteur |
| Messoudi Meriem | MRA | CRTI Cheraga Alger | Co-Rapporteur |
| Haddef Zakaria | MCA | University of Skikda | Examiner |

Academic Year : 2024/2025

# Acknowledgments

All praise and gratitude be to Allah, who granted me the patience, strength, and determination to complete this work.

This thesis was carried out under the supervision of **Dr. Kameli Kenza**, from the University of Skikda – 20 Août 1955. I would like to express my deepest and most sincere gratitude to her. She has been not only an exceptional supervisor but also the best professor and mentor I have had throughout my academic journey. Her constant support, kind guidance, and invaluable help were essential to the completion of this thesis, and I will forever be thankful for the privilege of working under her supervision.

I am honored that **Dr. Boulkhessaim Salim**, from the University of Skikda – 20 Août 1955, accepted to preside over the jury. My sincere thanks go to him for his time and consideration.

I also extend my warmest thanks to **Dr. Haddef Zakaria**, from the University of Skikda – 20 Août 1955, for accepting to examine and evaluate this thesis with interest and care.

My gratitude also goes to **Dr. Massoudi Mariem**, from CRTI – Chéraga, Algiers, for her participation in the jury and for her valuable insights.

A special thank you goes to **Hani Hadjoudja**, whose significant support and presence meant a lot to me. He stood by me not only as a cousin but also as a true brother. His encouragement and help were invaluable during difficult moments.

I would also like to sincerely thank every professor who illuminated my path during my studies. Each one of them left a positive mark on my academic and personal growth.

Finally, my heartfelt thanks to everyone who, in one way or another, contributed to the realization of this work – especially my beloved parents.

**Hadjoudja Ghofrane**

# *Dedication*

***In the name of Allah, the Most Gracious, the Most Merciful, the One and Only—by His grace, I have reached this moment of success. All praise and thanks are due to the Lord of all worlds.***

*To the dearest and most beloved family, from the eldest to the youngest, especially* ***my wonderful mother*** *and* ***my precious father****, who never withheld anything from me Those who lit and paved my path and*

*were always my greatest source of strength and support.*

*To* ***my beloved siblings****: Zaki, Yahia, and Malak, who have always been there for*

*me—with special thanks to* ***my brother Zakaria****, whose support meant the world.*

*To* ***the best aunts in the world****, who never hesitated to help and stood by me at every step. And to* ***my dear grandfather and grandmother****, who always dreamed of seeing me reach this day and supported me endlessly.*

*To* ***my dear uncles****, who have always been by my side since the beginning of my academic journey, and to* ***my cousins****, who felt more like siblings:* ***Alaa, Maysa, Hanaa…*** *and especially* ***Hani****, who has truly been like a brother to me.*

*To* ***Fatiha*** *and* ***Ilham*** *, who were like second mothers to me, just like my own aunts, during my stay at the university dormitory.*

*To* ***Roufiya****, the best friend I found during my hardest times—she was the light in my darkness. Thank you, my dearest, for being a constant and comforting presence.*

*To* ***Aya****, my safe space and the keeper of my secrets—your friendship has been a quiet source of strength and peace throughout this journey.*

*To all my other dear friends:* ***Khadija, Rania, Amal, Hania, Zeina, Maria, Ritaj, Imane****,****Nadjela …*** *and many others—thank you for being part of my journey.*

*To everyone who stood by me in difficult times, and to all who walked this path with me—through its joys and hardships—to all who were a source of strength when I needed it most,*

***I dedicate this humble thesis.***

***Ghofrane***

**Abstract :**

This thesis discusses transparent conductive oxides (TCOs), which are materials with unique physical properties as they combine high electrical conductivity with optical transparency. Tin dioxide ($SnO_2$) is highlighted as an n-type semiconductor that has high electrical conductivity, visible light transparency, and a wide band gap ranging from 3.5 to 3.8 eV. These properties make it suitable for applications like gas sensors, transparent electrodes, and photocatalysis. To further improve its physical properties, doping with zinc and copper is carried out. The work also focuses on the deposition of $SnO_2$ thin films using spray pyrolysis, a technique chosen for its simplicity, low cost, and ability to produce uniform films in an oxygen-rich environment. The thesis is structured into three chapters: the first chapter presents a bibliographic study of TCOs and thin films, analyzing $SnO_2$ properties and its applications while introducing photocatalysis and the reasons for using $SnO_2$ in this study. The second chapter explains the experimental methods, including spray pyrolysis with the Holmarc device, steps for preparing thin films, and discusses doping and semiconductors. The third chapter presents a comparative study of the structural, optical, and electrical properties of pure and Cu, Zn-doped $SnO_2$ thin films .

**Keywords** : $SnO_2$, thin films, spray pyrolysis, substrate temperature, characterization, transparent electrodes

**الملخص :**

تتناول هذه المذكرة أكاسيد التوصيل الشفافة(TCOs) ، وهي مواد تتميز بخواص فيزيائية فريدة تجمع بين الموصلية الكهربائية العالية والشفافية الضوئية. يُبرز البحث ثاني أكسيد القصدير ($SnO_2$) كأحد أشباه الموصلات من النوعn ، إذ يتميز بموصلية كهربائية عالية وشفافية في مجال الضوء المرئي وفجوة طاقة واسعة تتراوح بين 3.5 و3.8 إلكترون فولت، مما يجعله ملائمًا لتطبيقات مثل حساسات الغازات، الأقطاب الشفافة، والتطبيقات الضوئية التحفيزية. ولتحسين خصائصه الفيزيائية، يتم تطعيمه بالزنك والنحاس. يركّز العمل أيضًا على ترسيب أغشية رقيقة من $SnO_2$ باستخدام تقنية الانحلال الحراري بالرش، التي تتميز ببساطتها وتكلفتها المنخفضة وقدرتها على إنتاج أغشية متجانسة في بيئة غنية بالأوكسجين. تنقسم المذكرة إلى ثلاثة فصول: يعرض الفصل الأول دراسة بيبليوغرافية حول TCOs والأغشية الرقيقة، ويحلل خصائص $SnO_2$ وتطبيقاته، ويقدّم لمحة عن التحفيز الضوئي وأسباب استخدام $SnO_2$ في هذا البحث. يشرح الفصل الثاني الطرق التجريبية، بما في ذلك تقنية الانحلال الحراري بالرش باستخدام جهازHolmarc ، وخطوات تحضير الأغشية الرقيقة، ويتناول مواضيع التطعيم وأشباه الموصلات. أما الفصل الثالث فيقدّم دراسة مقارنة للخصائص التركيبية، البصرية، والكهربائية لأغشية $SnO_2$ النقية والمطعمة بالزنك والنحاس.

**الكلمات المفتاحية** : $SnO_2$ ، الأغشية الرقيقة، الانحلال الحراري بالرش، درجة الحرارة، الأقطاب الشفافة، التشخيص.

# LIST OF TABLES

# LIST OF FIGURES

## CHAPTER I

## CHAPTER II



## CHAPTER III

# LIST OF ABBREVIATIONS

| Symbole | Description |
|---|---|
| TCO | Transparent conducting oxides |
| CuO | Copper oxide |
| PVD | Physical Vapor Deposition |
| CVD | Chemical Vapor Deposition |
| MBE | Molecular Beam Epitaxy |
| PLD | Pulsed Laser Deposition |
| APCVD | Atmospheric Pressure Chemical Vapor Deposition |
| LPCVD | Low-Pressure Chemical Vapor Deposition |

## LIST OF ABBREVIATIONS

| | |
|---|---|
| MOCVD | Metal Organic CVD |
| PACVD | Plasma Assisted Chemical Vapor Deposition |
| CBD | Chemical bath deposition |
| XRD | X-RayDiffraction |
| d(hkl) | Inter-Plane Distance of Atomsor Ions or Molecules |
| n | Order of reflection |
| $\vartheta$ | Bragg angle |
| $\lambda$ | Photon wave length |
| $\beta$=FWHM | Full width at the half maximum of the XRD peak |
| D | Crystallite size |
| d | Inter plan arspacing |
| a,b,c | Lattice constants |
| $o$ | Microstrain |
| $\delta$ | Dislocation density |
| $N_0$ | number of crystallites |
| t | thickness |
| UV | Ultraviolet |

# LIST OF ABBREVIATIONS

| | |
|---|---|
| UV-Vis | Ultraviolet-visible |
| v | Frequency of photon |
| h | Planck's constant |
| hv | Photon Energy |
| Eg | Gap Energy |
| $\alpha$ | Absorption co-efficient |
| A | Absorbance |
| T | Transmittance |
| R | Reflectance |
| $\rho$ | Electrical resistivity |
| V | Voltage |
| I | Current |

# CONTENTS

CONTENTS



**II : Tin Oxide thin films Elaboration**

# INTRODUCTION

Transparent conductive oxides (TCOs) present a specific group of materials that have unique physical properties compared to other materials, they can combine many properties at the same time, such as; a high electrical conductivity and optical transparency in the visible range, mobility, bandgap, and a low refractive index **[01]** , among the most important TCOs are ZnO **[02]** , TiO2 **[03]** , Sb2O3 **[04]** , In2O3 **[05]** , and $SnO_2$ **[06-07]** .

Tin dioxide in general is an n-type semiconductor **[08]** and has many specific properties that can distinguish it compared to the other TCOs, from them: high electrical conductivity, transparency in the visible region, reflectivity in the infra-red region, and wide band gap (ranges between 3.5 and 3.8 eV) **[09-10]** , made it the most uses it in many applications, some of them: gas sensors **[11]** , solar cells **[12]** , transparent electrodes **[13]** , photocatalytic application…..etc.

Several effects can be applied on pure tin dioxide to further improve its physical properties, among them the doping effect. The elements used as dopants include cobalt, aluminum, gadolinium, zinc, and copper **[14-15]** . In this work, the last two elements will be used as dopants .

$SnO_2$ thin films can deposited using numerous techniques include: chemical vapor deposition (CVD) **[16]** , sol gel spin coating **[17]** sol gel dip coating **[18]** , pulsed laser deposition (PLD) **[19]** , and spray pyrolysis (SPT) **[20-21]** . Among the different deposition processes that we mentioned, spray pyrolysis is the most suitable one for preparing tin dioxide thin films, because of its simplicity and low cost **[22-23]**, homogeneity of the deposited films, and deposition in oxygen-rich air instead of

vacuum, which is more suitable for the preparation of thin film oxides, it also has the advantage of good control for the doping rate .

This thesis is divided into three chapters arranged as follows :

In **The first chapter** consists a bibliographic analysis of transparent conductive oxides (TCOs) We will also go over thin films and the different techniques that can be used to deposit them. The next parts will examine tin dioxide through a bibliographic analysis, showcasing its many qualities, such as its optical , electrical, and magnetic traits. Additionally, the uses of $SnO_2$ will be discussed. In addition, the chapter will give a succinct overview of the use of photocatalysis, the reasoning behind the choice of $SnO_2$ , and the main goal of our work in the paragraphs that follow .

In **The second chapter**, the experimental procedure is presented, beginning with an overview of the spray pyrolysis technique and the reasons for choosing it to deposit $SnO_2$ thin films. The Holmarc apparatus used in the process is described, along with the preparation of precursor solutions, including the chemical reagents and conditions applied. The chapter also introduces the characterization techniques and analytical equipment used to study the structural, optical, and electrical properties of the films.

In **The third chapter** is a comparative study between the structural properties (texture coefficient, lattice parameters and unit cell volume, crystallite size, microstrain, and dislocation density), surface morphologies, optical properties (transmittance, band gap, and Urbach energy values), and electrical properties (sheet resistance and electrical conductivity) of pure and Cu, Zn-doped tin dioxide thin films.

# References

**[01]** G. T. Chavan, Y. Kim, M. Q. Khokhar, S. Q. Hussain, E.C. Cho, J. Yi 2, Z. Ahmad, P. Rosaiah, C. W. Jeon, A Brief Review of Transparent Conducting Oxides (TCO): The Influence of Different Deposition Techniques on the Efficiency of Solar Cells, Nanomaterials. 13 (2023), 1226,

http:// doi.org/10.3390/nano13071226.

**[02]** M. Gartner, H. Stroescu, D. Mitrea, M. Nicolescu, Various Applications of ZnO Thin Films Obtained by Chemical Routes in the Last Decade, Molecules. 28 (2023), 4674, https://doi.org/10.3390/molecules28124674.

**[03]** O. B. khetta, A. Attaf, A. Derbali, H. Saidi, A. Bouhdjer, M. S. Aida, Y. B. khetta, R. Messemeche, R. Nouadji, S. Rahmane, N. E. Djehiche, Precursor concentration effect on the physical properties of transparent titania (Anatase-TiO2) thin films grown by ultrasonic spray process for optoelectronics application, Optical Materials. 132 (2022), 112790, https://doi.org/10.1016/j.optmat.2022.112790.

**[04]** A.S. Hassanien, I.M. El Radaf, Effect of fluorine doping on the structural, optical, and electrical properties of spray deposited Sb2O3 thin films, Mater. Sci. Semicond. Process. 160 (2023), 107405, https://doi.org/10.1016/j.mssp.2023.107405.

**[05]** A. Khan, E. Rahman, R. Nongjai, K. Asokan, Role of deposition temperature and Sn content on structural, optical & electrical properties of In2O3 thin films, Curr. Appl. Phys. 38 (2022) 49–58, https://doi.org/10.1016/j.cap.2022.03.004.

**[06]** I. Saoula, C. Siad, A. Ouahab, N. Allag, A. Chala, S. Rahmane, S. Marmi, N. Saheb, Synthesis and properties of alkaline earth elements (Ca, Sr, and Ba)

doped SnO2 thin films, Optical Materials. 145 (2023), 114372, https://doi.org/10.1016/j.optmat.2023.114372.

**[07]** P. Sivakumar, H.S. Akkera, T.R.K. Reddy, Y. Bitla, V. Ganesh, P.M. Kumar, G. S. Reddy, M. Poloju, Effect of Ti doping on structural, optical and electrical properties of SnO2 transparent conducting thin films deposited by sol-gel spin coating, Opt. Mater. 113 (2021), 110845, https://doi.org/10.1016/j. optmat.2021.110845.

**[08]** D. Filatova, M. Rumyantseva, Additives in Nanocrystalline Tin Dioxide: Recent Progress in the Characterization of Materials for Gas Sensor Applications, Materials. 16 (2023), 6733,https://doi.org/10.3390/ma16206733.

**[09]** E.C. Nwanna, P.E. Imoisili, T.C. Jen, Synthesis and characterization of SnO2 thin films using metalorganic precursors, J. King Saud Univ. Sci. 34 (2022), 102123, 4https://doi.org/10.1016/j.jksus.2022.102123.

**[10]** A.A. Dakhel, Study of structural, optical and magnetic properties of hydrogenated Ni and (Ga, Zn) co-doped SnO2 nanocomposites, Mater. Chem. Phys. 252 (2020), 123163, https://doi.org/10.1016/j.matchemphys.2020.123163.

**[11]** A. Thomas, L. Thirumalaisamy, S. Madanagurusamy, K. Sivaperuman, Incompatibility of Pure SnO2 Thin Films for Room-Temperature Gas Sensing Application, ACS Omega. 8 (2023), 32848-32854, https://doi.org/10.1021/acsomega.3c04038.

**[12]** P. Lisnic, L. Hrostea, L. Leontie, M. Girtan, Fluorine-Doped SnO2 Thin Films in Solar Cell Applications. Morphological, Optical and Electrical Properties, Arch. Metall. Mater. 68 (2023), 483-490, https://doi.org/10.24425/amm.2023.142426.

**[13]** R. Ramarajan, N. Purushothamreddy, R.K. Dileep, M. Kovendhan, G. Veerappan, K. Thangaraju, D.P. Joseph, Large-area spray deposited Ta-doped SnO2 thin film electrode for DSSC application, Sol. Energy. 211 (2020), 547–559, https://doi.org/ 10.1016/j.solener.2020.09.042.

**[14]** M. L. Ayachi, M. Difallah, B. Benhaoua, Nonlinear optical properties of cobalt doped SnO2 thin films, Optic. 272 (2023), 170296, https://doi.org/10.1016/j.ijleo.2022.170296.

**[15]** K. Ravikumar, S. Agilan, M. Raja, L. Raja, B. Gokul, R. Ganesh, N. Muthukumarasamy, Design and fabrication of Al/Sr: SnO2/p-Si Schottky barrier diode based on strontium-doped SnO2 thin film, Mater. Res. Express. 6 (2019), 026413, https://doi.org/10.1088/2053- 1591/aaed89.

**[16]** K. Juraic, D. Gracin, M. Culo, Ž. Rapljenovic, J. R. Plaisier, A. Hodzic, Z. Siketic, L. Pavic, M. Bohac, Origin of Mangetotransport Properties in APCVD Deposited Tin Oxide Thin Films, Materials. 13 (2020), 5182,

https://doi.org/10.3390/ma13225182.

**[17]** S. T. Bahade, A. S. Lanje, S. J. Sharma, Synthesis of SnO2 Thin Film by Sol-gel Spin Coating technique for Optical and Ethanol Gas Sensing Application, Themed Section: Science and Technology. 3 (2017), 567-575, http://doi.org/10.1016/j.physb.2017.09.112.

**[18]** K. Selma, B. Salima, B. Seddik, R. Djamil, H. Lazhar, Investigation of UV photosensor properties of Al-doped SnO2 thin films deposited by sol-gel dip-coating method, Journal of Semiconductors. 44 (2023), 032801, https://doi.org/10.1088/1674-4926/44/3/ 032801.

**[19]** R. Kajal, A. Kandasami, B. Kataria, P. Solanki, D. Mohan, Structural, optical, and dielectric characteristics of pulsed laser deposited SnO2-TiO2 composite thin films, Physica Scripta. 98 (2023), 085935,http://doi.org/10.1088/1402-4896/ace569.

**[20]** B. Maharnavar, A. Pardeshi, M. Patil, P. Pingale, M. Padvi, M. Bagal, Effect of thermal treatment of the SnO2 thin film prepared by spray pyrolysis method, AIP Conference Proceedings. 2716 (2023), 020002, https://doi.org/10.1063/5.0130929.

**[21]** N. Katariya, B. Singh, A. Saxena, V. Ganesan, Effect of Carrier Gas on Spray Pyrolysis Deposited SnO2 Thin Films, Macromolecular Symposia. 407 (2023), 2100473, https://doi.org/10.1002/masy.202100473.

**[22]** A. Abdelkrim, S. Rahmane, O. Abdelouahab, N. Abdelmalek, G. Brahim, Effect of solution concentration on the structural, optical and electrical properties of SnO2 thin films prepared by spray pyrolysis, Optik. 127 (2016), 2653–2658, https://doi. org/10.1016/j.ijleo.2015.11.232.

**[23]** C. Khelifi, A. Attaf, H. Saidi, A. Yahia, M. Dahnoun, Investigation of F doped SnO2 thin films properties deposited via ultrasonic spray technique for several applications, Surface. Interface. 15 (2019),244–249, https://doi.org/10.1016/j. surfin.2019.04.001.

# CHAPTER I

***An Overview of Thin Films and $SnO_2$ Properties***

In this chapter will be provided a bibliographic analysis of transparent conductive oxides (TCOs) We will also go over thin films and the different techniques that can be used to deposit them. The next parts will examine tin dioxide through a bibliographic analysis, showcasing its many qualities, such as its optical, electrical, and magnetic traits. Additionally, the uses of $SnO_2$ will be discussed. In addition, the chapter will give a succinct overview of the use of photocatalysis, the reasoning behind the choice of $SnO_2$ , and the main goal of our work in the paragraphs that follow .

# I.Thin films

## I.1.Introduction

Thin film technology is simultaneously one of the oldest arts and one of the newest sciences. Involvement with thin films dates to the metal ages of antiquity. Consider the ancient craft of gold beating, which has been practiced continuously for at least four millennia . Gold's great malleability enables it to be hammered into leaf of extraordinary thinness while its beauty and resistance to chemical degradation have earmarked its use for durable ornamentation and protection purposes. The Egyptians appear to have been the earliest practitioners of the art of gold beating and gilding. Many magnificent examples of statuary, royal crowns, and coffin cases that have survived intact attest to the level of skill achieved **[01]** .

## I.2.Definition

Thin films are a substance deposited in another substance called a substrate. The layer is reduced to one of the dimensions (thickness) of this deposite, which ranges from nanometers fractions. This semi-second dimension gives the first characteristic of thin films, and more importantly, reversing materials in bulk film characteristics are generally affected by the conditions of preparation: Deposition method and criteria, substrate type…**[02]**.

## I.3.Stages of Thin Films Growth

In order to obtain fine quality thin films for device applications and for better understanding the properties, the concepts regarding the nature of the films should be

understood. The ideal condition of the film formation involves the deposition of the material atom by atom (or molecule by molecule) and layer by layer with proper time interval between the two successive depositions so that, they can occupy the minimum potential energy configuration with respect to the substrate and subsequently on the previously deposited layers **[03]**.

For more understanding thin films, the following properties illustrate various mechanisms occurring at different stages of film growth. There are several stages in the growth process, fromthe initial nucleation of the deposits to the final continuous three dimensional film formation states **[04]** :

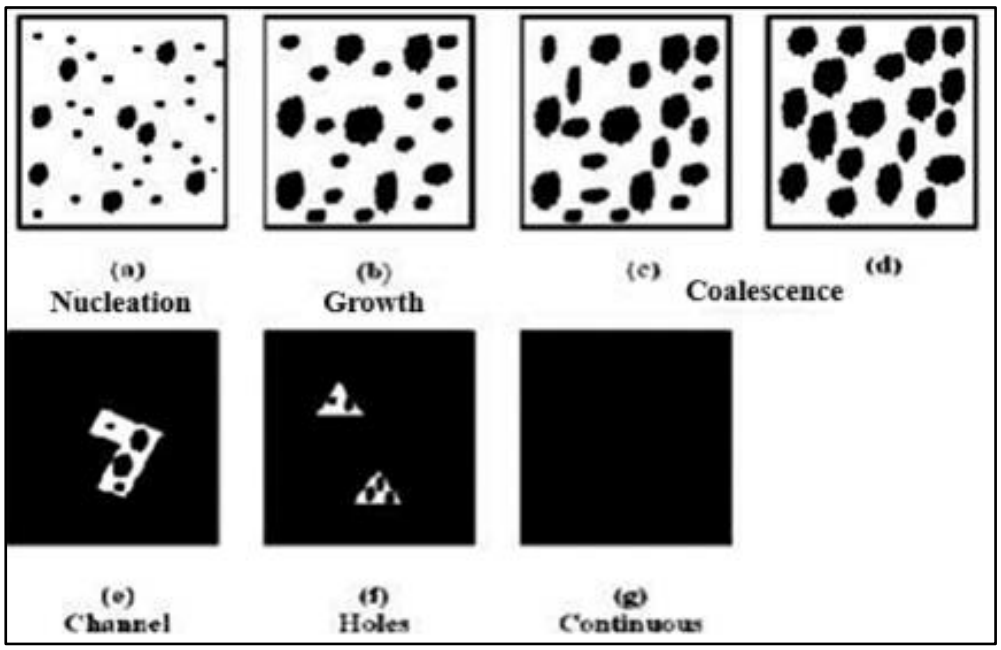


**FigureI.01 :***Schematic diagram showing stages of thin film growth* **[03]** .

**a) Nucleation**

The nucleation is the primary process for all deposition. The common process of addition, adsorption, desorption, migrations, etc. of atoms is called nucleation or small cluster formation which is schematically shown in (figureI.1-a) .

**b) Island structure**

The islands consist of comparatively larger nuclei (>10 Å) and generally of three dimensional natures with their height, however, much less than their lateral dimensions. The formation of these islands and their growth take place either by direct addition of atoms from the vapor phase or from other environment or by the

diffusion controlled process (see figureI.1-b). The diffusion controlled process is moreover commonly observed except at low substrate temperature.

**c) Coalescence**

As mentioned in the second stage, as islands grow they develop some characteristic shapes and then with further growth, coalesce with the neighboring ones by rounding off their edges near the joining region (neck) where these deposits assume a liquid like structure. The coalescence involves considerable transfer of mass between islands by diffusion. Small islands disappear rapidly. The process resembles the sintering of bulk powder where the individual particles assume spherical shapes due to the lowering of their surface energies. During coalescence of two islands which occurs at their necks recrystallisation as well as annealing takes place leading to some definite shapes of larger islands (figure I.1-c and d).

**d) Channel and Holes**

As the coalescence continues with deposition, there will be a resultant network of the film with channels in between (figureI.1-e). These channels do not remain void, but the secondary nuclei start to grow within these void spaces in the channel. Sometimes these channels may not be completely filled up even with increasing film thickness thus leaving some holes or gaps in the aggregate mass (see figureI.1-f). With increasing film thickness, these holes or gaps will decrease in size.

**e) Continuous film**

When these gaps are completely bridged by the secondary nuclei, films will be continuous. However, it often happens that some void space may still remain unbriged. In an ideal continuous film there should not be any gap in the aggregate mass. Such a stage in the filmcan be attained at certain average film thickness (figureI.1-g) **[03]**.

## I.4.Methods for the preparation of $SnO_2$

Applications for thin film processing are numerous. The most widely used processes for $SnO_2$ thin films are molecular-beam epitaxy, chemical vapor deposition (CVD), metalorganic chemical vapor deposition (MOCVD), and pulsed laser

deposition (PLD).High performance $SnO_2$ materials can be produced with these processing settings.

New processing methods include chemical spray pyrolysis, screen printing, electrochemical deposition, and sol-gel synthesis have gained popularity recently; the latter provides a low-cost, resource-efficient method **[05]** .

***TableI.1:*** *Methods of thin flms deposition* **[06]**.

| Physical deposition | Chemical deposition |
|---|---|
| **Evaporation techniques :**<br>- Vacuum thermal evaporation;<br>- Electron beam evaporation;<br>- Laser beam evaporation;<br>- Arc evaporation;<br>- Molecular beam epitaxy;<br>- Ion plating evaporation. | **Sol-gel technique** |
| | **Chemical bath deposition** |
| | **Spray pyrolysis technique** |
| | **Plating:**<br>- Electroplating technique;<br>- Electroless deposition. |
| **Sputtering techniques**:<br>- Direct current sputtering (DC sputtering);<br>- Radio Frequency sputering (RF sputtering). | **Chemical vapor deposition (CVD):**<br>- Low pressure (LPCVD);<br>- Plasma enhanced (PECVD);<br>- Atomic layer deposition (ALD). |

## I.4.1.Physical Vapour Deposition process (PVD)

A broad range of vapor-phase technologies are included in PVD processes, which are a general name for any of several techniques for depositing thin solid films onto different surfaces by condensing a vaporized version of the solid material. PVD entails the physical ejection of material in the form of molecules or atoms, followed by their condensation and nucleation onto a substrate.

Reactive deposition is the process by which gases supplied into the vapor undergo a chemical reaction with the vapor-phase material, which can be made up of ions or plasma, to create new molecules **[06]**.

### I.4.2.Chemical vapor deposition (CVD)

Although the previously stated physical methods for producing thin films provide good quality and functional features, they are quite costly and may require a significant quantity of material target. Chemical Vapor Deposition (CVD) is an extremely old processing method that dates back to the late 1800s .

High-purity refractory materials like zirconium and titanium were primarily produced using it. The majority of them don't require costly equipment. Researchers began observing the potential benefits of CVD after World War II, and its use and effectiveness grew **[07]** .

Precursors determine the film composition in these techniques, and stoichiometry can be reached by regulating the precursors and deposition rate. It doesn't need a high vacuum and can permit codeposition of elements. Thin films are grown using CVD methods at typical atmospheric circumstances. This method deposits semiconductor films, organic insulating films, and inorganic insulating films **[08, 09]**.

There are four key steps of a typical CVD process :

1. A thermal activation of the chemical precursors to form a vapor.
2. This vapor is then transported through a heated chamber where the substrate is located.
3. In this chamber, the desired gas phase reactions occur and the reactants are deposited onto the substrate surface resulting in film formation.
4. Volatile byproducts are desorbed from the film and removed from the chamber through convection.

### I.4.3.Pyrolysis spray technique (PS)

Pyrolysis spray is a processing technique being considered in research to prepare thin and thick films, ceramic coatings and powders . Unlike many other film deposition techniques, spray pyrolysis represents a very simple and relatively cost-effective processing method (especially with regard to equipment costs). It offers an extremely easy technique for preparing films of any composition. Spray pyrolysis does not require high-quality substrates or chemicals. The method has been employed

for the deposition of dense films, porous films and for powder production. Even multilayered films can be easily prepared using this versatile technique **[10]** .

### I.4.3.1. Classification of spray pyrolysis techniques

Spray pyrolysis is a versatile processing technique for preparation of dense and porous single and multilayered films and powders of various materials and morphologies.Classification of different spray processes could be made in one way based on the type of energy source for the precursor reaction; such as spray pyrolysis in a tubular reactor (SP), vapor flame reactor (VFSP), the emulsion combustion method (ECM) and flame spray pyrolysis (FSP); or the method of atomizing the precursor, namely air pressurized, electrostatic and ultrasonic spray pyrolysis. In the case that the energy source for precursor reaction is an external energy supply and not from the spray itself, (as in SP and VFSP), method is less sensitive to the choice of precursors and solvent **[11]** .

Different types of solvents are used in spray pyrolysis depending on the type and solubility of the precursors and economic aspects. Nitrates, chlorides and acetates are typically chosen as the metal oxide precursors that can be dissolved in aqueous and alcoholic solvents

The other classification for the type of spray pyrolysis is usually attributed to the type of the atomizer that is used in the system. In addition, the droplet size of the aerosol is generally dependent on the atomization method, which in turn determines the film quality. There are three major types of atomizers: air blast, electrostatic and the ultrasonic. The spray pyrolysis technique using the electrostatic atomizer is called Electrostatic Spray Deposition (ESD), the technique using the air blast atomizer is named Pressurized Spray Deposition (PSD) and the technique using

Ultrasonic atomizer is generally recognized as the ultrasonic or normal Spray Pyrolysis **[12]** .

**Table I.2:***Characteristics of atomizers commonly used in spray pyrolysis*

| Atomizer | Droplet size (µm ) | Atomization rate ( $cm^3/min$ ) |
|---|---|---|
| Pressure | 10 – 100 | 3 – no limit |
| Nebulizer | 0.1 – 2 | 0.5 – 5 |
| Ultrasonic | 1 – 100 | < 2 |
| Electrostatic | 0.1 – 10 | |

Thin film deposition using spray pyrolysis can be divided into four types of processes **[28]** that may occur during deposition are showing in Fig.I.2 :

- **In process 1:** the droplet splashes on the substrate, vaporizes and leaves a dry precipitate in which decomposition occurs.
- **In process 2:** the solvent evaporates before the droplet reaches the surface and the precipitate impinges upon the surface where decomposition occurs.
- **In process 3:** the solvent vaporizes as the droplet approaches the substrate then the solid melts vaporizes (or sublimes) and the vapor diffuses to the substrate to undergo a heterogeneous reaction there, this is true CVD.
- **In process 4:** at the highest temperatures the chemical reaction takes place in the vapor phase.

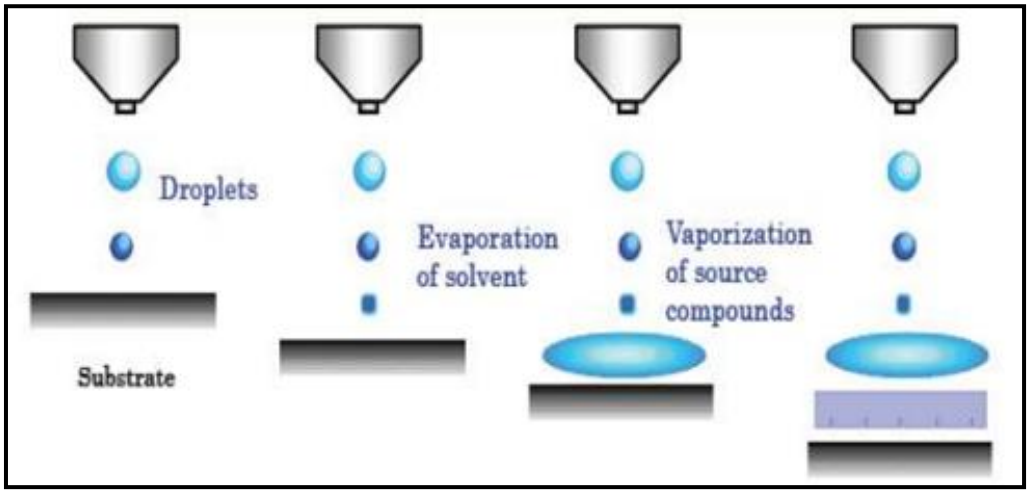


***Figure I .02 :*** *spray process* ***[13]*** .

## I.4.3.2.Advantages of spray pyrolysis

In comparison with other thin film deposition methods, spray pyrolysis has many advantages including: open-atmosphere process, open reaction chamber, easy access to observe the deposition process and adjustment during the experiment. It has

also the multi-layer fabrication capability, which is very attractive for making functionally graded films. The composition of the film can be adjusted by changing the precursor solutions. Films can be also obtained on large surfaces at temperatures ~ 500 °C. One of the major advantages of spray pyrolysis over the vapor phase routes is the possibility of producing multi component particles with exact desirable stoichiometry in the final product. Depending on the substrate temperature, precursor type and the nozzle-substrate distance, the droplets can evaporate or decompose completely before reaching the substrate, resulting in a process resembling to CVD or the liquid is deposited without evaporation. Burning a flammable precursor may also result in forming a particulate spray or to obtain higher deposition temperatures **[12]** .

## I.4.4. Characterization techniques of thin films

### I.4.4.1.Energy dispersive X-ray spectroscopy

Energy Dispersive X-Ray Spectroscopy was used for the elemental analysis and chemical characterization of a sample. Compositional homogeneity of the film was also analyzed via recording the composition maps **[12]** .

### I.4.4.2.X-ray diffraction

X-ray diffraction has been used to identify the crystalline phases of the materials based on the Bragg's law. As shown in ( Fig I.3.A ) , condition at which diffraction occurs in a crystalline material satisfying the Bragg's law is described as **[14]** :

$$n\lambda = 2dsin\theta \qquad \textbf{(I…1)}$$

Where :**λ** is the wave length of the X-ray beam; **d** is the spacing between the planes in the atomic lattice; **θ** is the angel between the incident ray and the scattering planes;

**n** is the order of diffraction.

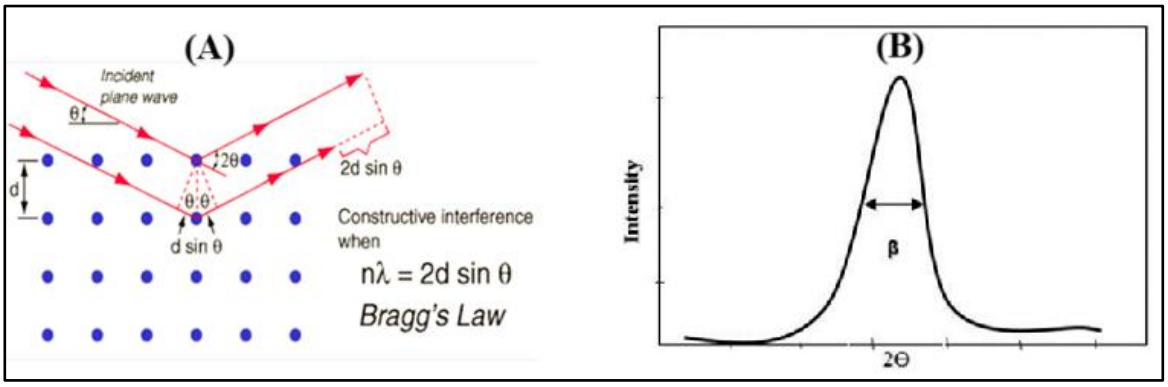


**Figure I.3 :***(A) Bragg's law, (B) Full width at half maximum.*

**a) Determination of the grains size**

The of crystallites was calculated using a well-known Scherrer's formula **[15]** :

$$\mathbf{D} = \frac{K\lambda}{\beta cos\theta} \qquad \textbf{(I...2)}$$

Where: **K** is Constant **D** is the of crystallite, **λ** (=1.5405 Å) used the wavelength of X-rays,**β** the broadening of diffraction line measured at half maximum intensity in radians (Fig.I.3.B) and **θ** is the angle of diffraction.

## I.4.5.Optical characterization and measurement

### I.4.5.1. Ultraviolet visible spectroscopy

Ultraviolet visible spectroscopy or ultraviolet-visible spectrophotometry (UVVis or UV/Vis) refers to absorption spectroscopy or reflectance spectroscopy in the ultraviolet visible spectral region. The absorption or reflectance in the visible range directly affects the perceived color of the chemicals involved, it measures the intensity of light passing through a sample **(I)** and compares it to the intensity of light before it passes through the sample **($I_0$)**. The ratio **( $\frac{I}{I_0}$ )** is called the transmittance and it is usually expressed as a percentage **(T %)**. The absorbance, A is based on the transmittance **[16]**:

$$A = -\log(\frac{T}{100\,\%}) \qquad \textbf{(I…3)}$$

The UV-visible spectrophotometer can be also configured to measure reflectance. In this case, the spectrophotometer measures the intensity of light

reflected from a sample **(I)**, and compares it to the intensity of light reflected from a reference material **($I_0$)** (such as a white tile).

The ratio **( $\frac{I}{I_0}$ )** is called the reflectance, and is usually expressed as a percentage (R %) **[16]**.

### I.4.6.1. Film thickness

#### a) Swanepoelmethod

Thickness of deposited samples prepared at different solution flow rates and at different doping was calculated using modified Swanepoel envelop method (an envelope was drawn using the maxima and minima of each curve and also used value of refractive index ns of quartz glass was 1.52) Fig.I.4 , **[17]** , the film thickness:

$$t = \frac{\lambda_1 \lambda_2}{2(\lambda_1 n_2 - \lambda_2 n_1)} \qquad \textbf{(I…4)}$$

Where $\lambda_1$ and $\lambda_2$ are the wavelengths at which two successive maxima or minima occur and $n_1$ and $n_2$ are the corresponding refractive indicesn **[18]** :

$$n = [N + (N^2 - n_s^2)^{1/2}]^{1/2} \qquad \textbf{(I…5)}$$

Moreover, **N** obtained by this relation **[15]** :

$$N = 2n_s^2 \frac{(T_M - T_m)}{T_M T_m} + \frac{(n_s^2 + 1)}{2} \qquad \textbf{(I…6)}$$

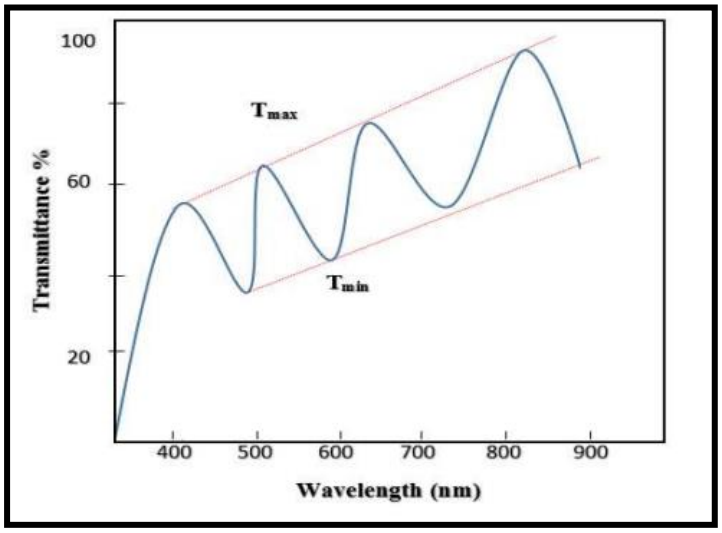


***Figure I.4 :*** *Method of interference fringes to determinate the thickness*

### b) Band gap

The measurement of the band gap of materials is important in the semiconductor, nanomaterial and solar industries. This note demonstrates how the band gap of a material can be determined from its UV absorption spectrum.

The term **"band gap"** refers to the energy difference between the top of the valence band to the bottom of the conduction band (Fig.I.5); electrons are able to jump from one band to another. In order for an electron to jump from a valence band to a conduction band, it requires a specific minimum amount of energy for the transition, the band gap energy. A diagram illustrating the band gap is shown in Fig. I.5.a **[20]** .

The band gap energy of insulators is large (> 4eV), but lower for semiconductors (< 3eV).

From the transmittance spectrum in the UV-visible the variation of $(\alpha h\nu)^2$ with photon energy hυ for thin film is shown in Fig.I.5.b. It has been observed that the plots of $(\alpha h\nu)^2$ versus hυ are linear over a wide range of photon energies indicating the direct type of transitions. The intercepts (extrapolations) of these plots (straight lines) on the energy axis give the energy band gaps **[15]** .

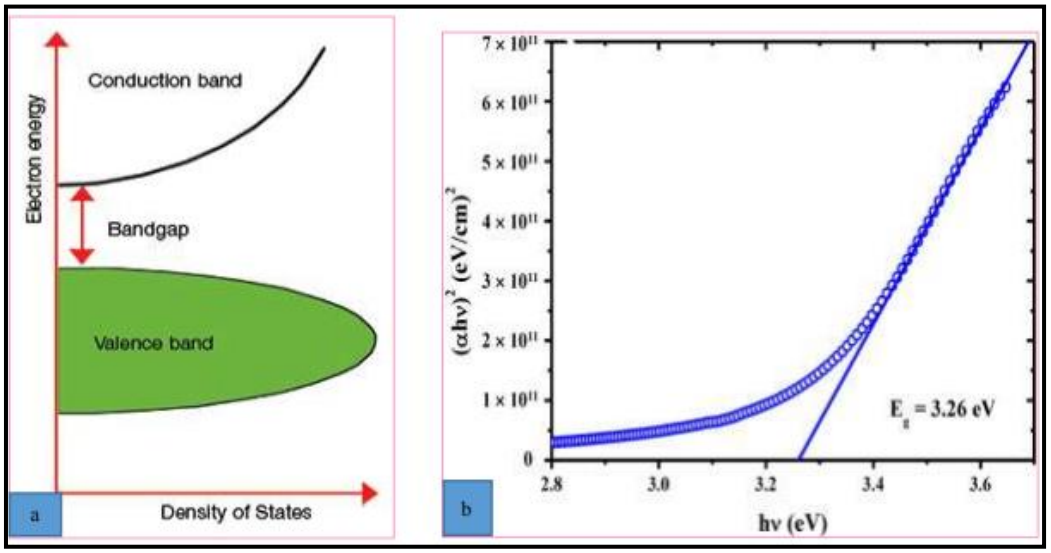


***Figure I.5 :*** *Explanation of band gap* ***[20]*** .

### c) Disorder calculating (Urbach Energy)

Ultrasonic Spray Pyrolysis is a deposition method which growth of the film is by condensation. In this situation, the atoms arriving on the substrate can stick to the point of landing. Therefore, the atoms in the film of the network are not usually in an ideal position, hence, the appearance of the gaps in the width of the $SnO_2$ bond, in this case, the strip edges disclosed in the case of crystal lattices and delimited by Ev and Ec may disappear. We observe localized states formed band tails border of the band gap in the valence band and conduction. For energies above and below Ev, Ec are the extended states, this difference known as the disorder or Urbach Energy; According to Urbach law, the absorption coefficient **α** is **[21]** :

$$\alpha = \alpha_0 \exp \frac{h\nu}{E_{00}} \qquad \textbf{(I…7)}$$

By plotting (Lnα) as function of hν (Fig. I.6) we can determine the value of

$$E_{00}\, Ln\alpha = Ln\alpha_0 + \frac{h\nu}{E_{00}} \qquad \textbf{(I…8)}$$

Wher$E_{00}$: is Urbach energy, which determine disorder .

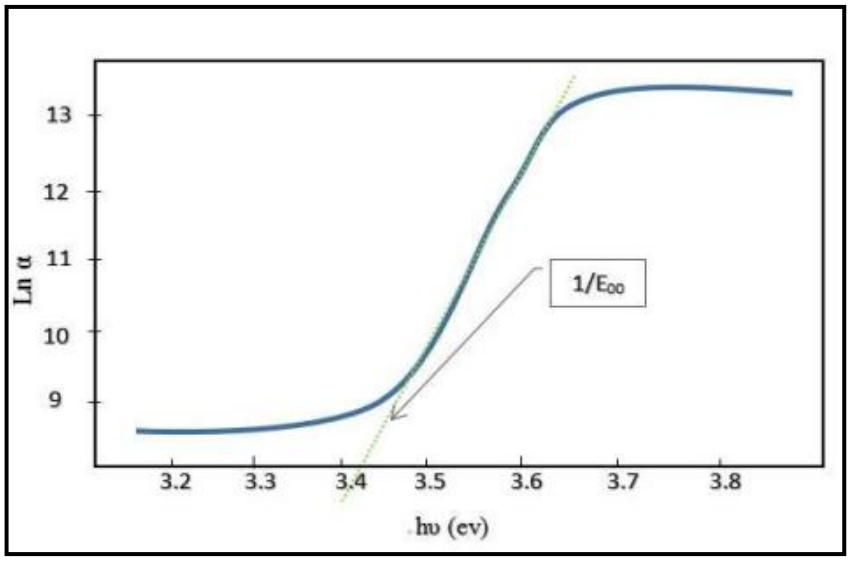


***Figure I.6 :*** *Urbach Energy Determination .*

### I.4.6.2.Determination of the film thickness by using Gravimetric Method

These method based on the determination of mass. The film thickness t can be calculated from the mass of the coating m if the density ρ and the area A on which the material is deposited are known :

$$t = m/A\rho \quad \textbf{(I…9)}$$

For this method, one has to bear in mind that the density of a coating may deviate significantly from that of the bulk (e.g. due to porosity or implanted interstitial atoms). For exact measurements, calibration is necessary **[19]**.

## I.5.Electrical characterization

### I.5.1.Hall effect

Hall effect measurements are important to semiconductor material characterization The designed automatic measuring system can be used to determine several material parameters: Hall coefficient ($R_H$ ), type (n or p), carrier concentration (n), the Hall voltage ($V_H$ ) and the conductivity are all extracted from the Hall voltage measurement. In order to obtained carrier mobility (μ) it is needful to measure also the resistivity of the sample ($\rho$) . Due to the required contact node arrangement shown in FigureI.7.a, a contact configuration gives current and voltage perpendicular to each other .

The van der Pauw method has been extensively used, to calculate the sample resistivity in the Hall measurement apparatus, the Hall voltage can be measured using the configurations shown in figure I.7.b. For ideal square symmetry samples the measured voltage at zero magnetic field should be 0 independently of the used current **[22,23]**.

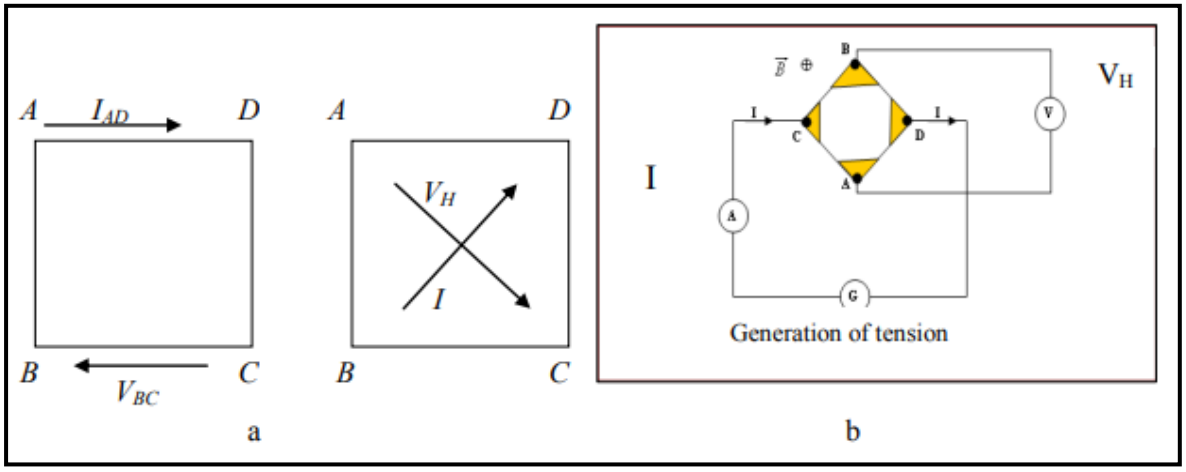


***Figure I .7 :*** ***a****-contact node arrangement,* ***b****-schemat shows hall volage measurement,*

For Hall effect measurements, a voltage is applied between the contacts placed at diagonally opposite corners and the current I flowing between them is measured.

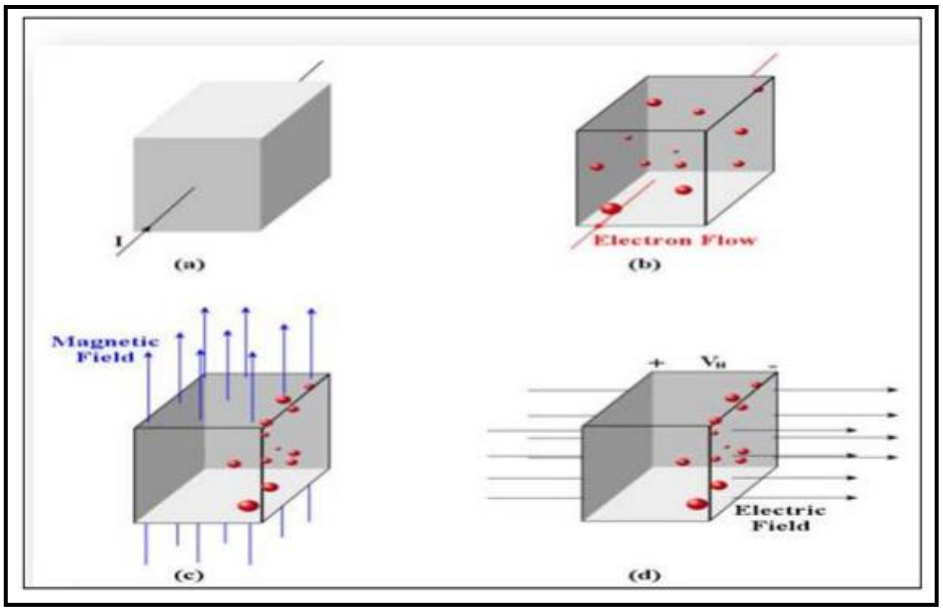


***Figure I .8 :*** *The Hall effect (a) - a current flowing through a piece of semiconductor material, (b) - the electrons flowing due to the current, (c) - the electrons accumulating at one edge due to the magnetic field, and (d) - the resulting electric field and Hall voltage* $\boldsymbol{V_H}$

In addition, a magnetic field B is applied in the direction perpendicular to the sample and the change in Hall voltage $V_H$ between the contacts in opposite corners is measured. Resistivity $\rho$ , carrier density n, and mobility μ are calculated from the measured values, applied magnetic field B and the film thickness d of the measured sample **[24]**. The Hall effect systeme is shown in figure I.9.

From the Hall voltage measurements it is possible to determine Hall coefficient using equation :

$$R_H = \frac{V_H\, d}{I\, B} \qquad \textbf{(I…10)}$$

Also we can specify the type of semiconductor (n or p) by the sign of the ($B \cdot R_H$),

where:

$B \cdot R_H$ <.....we have P-type semiconductor

$B \cdot R_H$ >.....we have N-type semiconductor

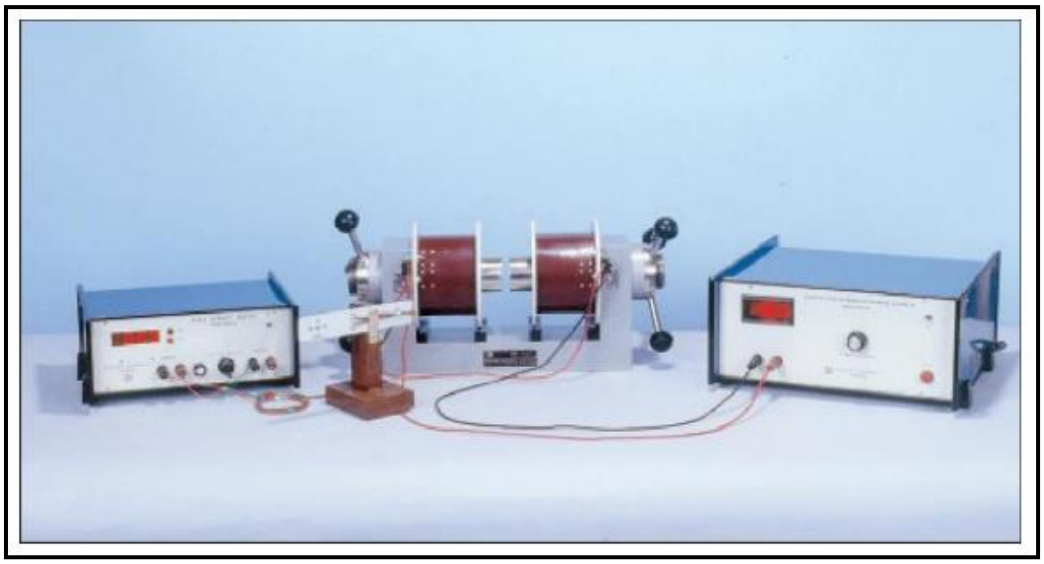

***FigureI.9 :*** *The hall effect system .*

And consequently carrier concentration can be determined.

$$n = \frac{1}{R_H\, q} \qquad \textbf{(I…11)}$$

Where q is the elementary charge. Finally, Hall coefficient and resistivity are used to determine hall mobility.

$$\mu = \frac{R_H}{\rho} \qquad \textbf{(I…12)}$$

For getting a well accuracy of obtained parameters it is necessary to ensure some basic conditions during the measurement. The most crucial one is to have good ohmic contacts.

Very important is also to ensure negligible heating of the sample during the measurements, sensitive current measurement, and good symmetry and homogeneity of the sample .

## II.Transparent conductive oxide

### II.1.Definition

A best transparent conductive oxide is known by its high transparency in the visible region and high electrical conductivity, and this is achieved whenever the conditions of preparing thin film are controlled very well (time of deposition, temperature….) which leads to reducing the structural defects. According to the energy band theory, three electrical states are possible: conductor, insulator, and semiconductor. In the conductor, the conduction band ($C_B$) and the valence band ($V_B$) overlap, thus allowing the free flow of electrons, the semiconductor has, for its part, a forbidden band that separates $V_B$ and $C_B$ commonly called gap and noted by optical energy, the electrons cannot take the energies located in this bandaged. They need to acquire energy to move into the $C_B$. For a gap greater than 4 eV, we speak of insulation because even at room temperature, $C_B$ is empty **[25]**. So, the TCOs can be classified as n-type degenerate semiconductors.Moreover, In recent years, a few p-doped TCOs have been studied **[26,27]**.

There are many factors for choosing the TCO among them the figure of merit Φ or Q which was built by Haacke in 1976, this factor is a correlation between optical properties and electrical properties which is given by the following relationship **[25,28]** :

$$\Phi = \frac{T^{10}}{R_{sh}} \qquad \textbf{(I…13)}$$

$$Q = \frac{\sigma}{\alpha} = \frac{1}{R_{sh}.\ln(R+T)} \qquad \textbf{(I…14)}$$

where T (%) is the total transmittance in the visible region, R (%) the total reflectivity, α ($cm^{-1}$) the absorption coefficient, σ $(\Omega.cm)^{-1}$ the electrical conductivity, and $R_{sh}$ (Ω/□) is the sheet resistance. From the most attractive TCOs are : $SnO_2$ **[29]**, ZnO **[30]**, and $TiO_2$ **[31]**,...etc .

## II.2.Transparent conductiveoxides (OTC) properties

### a) Electricalproperties

The electrical properties of transparent conductive oxides are very sensitive to oxygen sub - stoichiometry as well as to the nature and concentration of impurities introduced into the material by doping, in most cases, we get n-type TCO if dopants used are generally of higher valence than that of the substituted atoms, which leads to providing free electrons and are considered to be centres donors, so the electrical conductivity increase **[32]**.

### b) Optical properties

The optical properties of materials are governed by three essential phenomena which are transmission (T), reflection (R), and absorption (A), but for the TCOs the transmission is the most important optical property that determines their quality, is defined as the ratio of the intensity of light transmitted '$\boldsymbol{I_T}$' through a material divided to the intensity of light incident on its surface '$\boldsymbol{I_0}$':

$$T = I_T/I_0 \qquad \textbf{(I…15)}$$

$$T\ (\%)\ = 100.T \qquad \textbf{(I…16)}$$

A typical representation of the transmission spectrum of a TCO is presented in Figure I.19

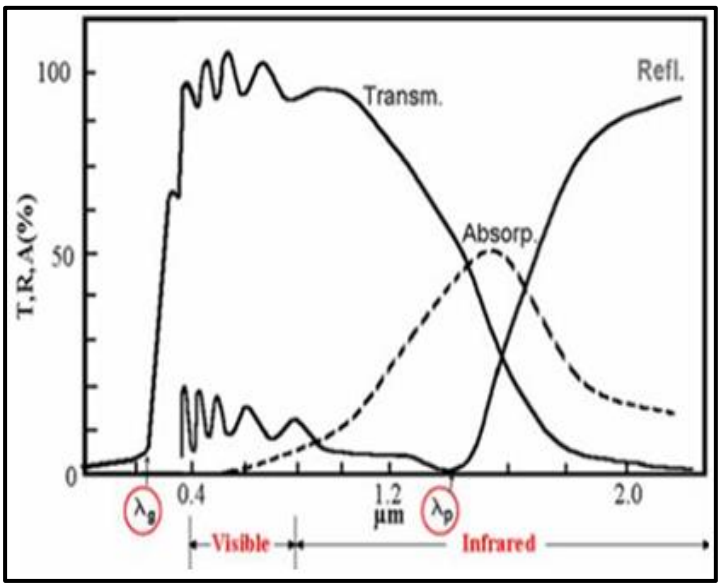


**Figure I.10 :** *Transmission, reflection and absorption factors of a conductive transparent oxide* **[33]** .

As can be seen in the figure, the transmission of a TCO is limited by two wavelengths (λg and λp), so we have three cases:

- ✓ **λ<λg:** this is the ultraviolet domain of wavelengths, the energy of photons that is greater than or equal to that of the gap is absorbed and the electrons are transferred from the valence band into the conduction band. It is the band-to-band transitions that dominate in this case.
- ✓ **λg <λ<λp :**the conductive oxide is transparent throughout this range which encompasses visible and near-infrared wavelengths. The transparent conductive oxide acts as a conductive anti-reflective layer
- ✓ **λ ≥ λp :** in the near-infrared (above 1200 nm), the TCO does not transmit more light. In thisinterval, TCO exhibitsstrongabsorption.

## III.Tin dioxide ($SnO_2$)

### III.1.Definition

Transparent conductive oxides are considered thin films and can be used in many applications depending on the oxide used, the most important of which is tin dioxide ($SnO_2$), as it is in the form of a thin layer that has a high optical transmittance greater than 90% and high electrical conductivity **[34]**, and wide band-gap (3.6 eV) **[35]**, it also has many other advantages, such as economical, chemically stable,

innocuous, mechanical stable **[36]** . Table I.3represents a general physical properties of the $SnO_2$.

**Table I.3 :** *Physical property of $SnO_2$* **[37]**.

| Property | Value |
|---|---|
| **Molar mass (g/v)** | **150.70** |
| **Specificdensity (g/Cm)** | **6.915** |
| **Melting point (C°)** | **1630** |
| **Boiling point (C°)** | **2330** |
| **Hardness** | **7.8** |

## III.2.Crystallin structure

Tin dioxide has a rutile structure (Figure I.20). The unit cell is generally (tetragonal) quadratic (a = b = 0.475 nm and c = 0.318 nm) and contains six atoms : two tin atoms and four oxygen atoms, each tin atom is in the centre of a nearly regular octahedron formed by six oxygen atoms, while each oxygen atom is surrounded by three tin atoms located at the vertices of an isosceles triangle. Oxygen is in position 4f (space group P42 / mmm) given by (u; u; 0), (1-u; 1-u; 0), (1/2 + u; 1/2- u; 1/2) and (1/2-u; 1/2 + u; 1/2) with u = 0.31. Tin is located: (1/2; 1/2; 1/2) and (0; 0; 0). The ionic radii of the $Sn^{4+}$cation and the $O^{2-}$ anion are respectively 0.71 °A and 1.40 °A **[38]**.

However, $SnO_2$ has been observed that under fairly high pressures, it can crystallize in an orthorhombic structure **[39]**.

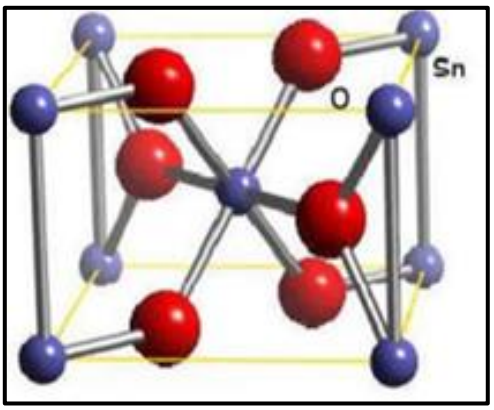


**Figure I.11 :** *Tin oxide unit cell (Rutile type structure).*

It is crucial to remember that the crystallinity and, consequently, the crystallographic orientation of the layers depend on the production temperature, the production techniques, and the doping rate. The authors' convention is that the preferential orientation in (101) or (110) varies depending on the method of tin oxide production **[40,41]** .

## III.3.Optical properties

Tin dioxide has an important reflection of infrared rays and high absorption in the ultraviolet range however its transmittance is more than 80% in the visible region **[42]**, so the undoped $SnO_2$ has high transmittance in the visible region because of the few crystal defects, but when it doped with some different elements, free electrons are formed and a transition level energy created in the bandgap so it narrows as representing in Table 2. Figure I.12 shows the decrease in the optical transmittance of $SnO_2$ thin film when it is doped with different concentrations of "$S_r$", while the undoped has the highest value.

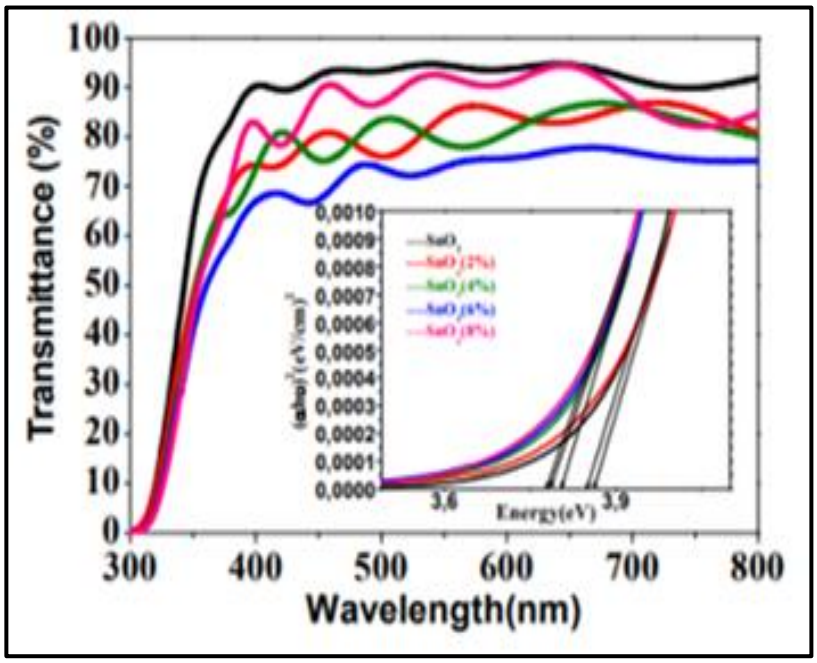


**Figure I.12 :***Optical transmittance spectrum of $SnO_2$ thin films prepared at different Sr doping concentration* **[43]**.

## III.4.Electrical properties

The characteristic electrical properties of $SnO_2$ are the resistivity of the films, the density of charge carriers, and their mobility. Several techniques can be used to measure the electrical properties such as : four-point method, and Hall effect .

Pure, monocrystalline $SnO_2$ tin dioxide is a semiconductor material with a large band gap energy ranging from 3.6 to 4.0 eV **[44]**.This intrinsic semiconductor is practically insulating (stoichiometric $SnO_2$) but once doped it becomes a relatively good conductor (non-stoichiometric) this case is called intrinsic doping it is the oxygen vacancies that generate electrons in the conduction band .

An oxygen vacancy is formed when an oxygen atom is removed from a normal site. It can be created under the impact of temperature. The oxygen vacancies exist in three different charge states: $V_o^0$ , $V_o^+$ , and $V_o^{+2}$ in the oxide **[45]**, also doping is achieved by introducing atoms from different columns generally III (like In), II (like Zn) **[44]** or V (like Sb) which has approximately the same ionic radii as the tin ions $Sn^{4+}$(0.071nm); (0.084 nm for $In^{3+}$ **[42]** ,0.088 nm for $Zn^{2+}$**[46]**, and 0.064 nm for $Sb^{5+}$**[47]**), also there are other elements it can be used to dope it like alkaline earth **[48]**.

Shallow donor levels for $V_o^+$ and $V_o^{+2}$ have been identified at 0.03 and 0.15 eV below the conduction band minimum (CBM), respectively. All these cases are close to the CBM so they will not cause a loss of transparency, but will enhance the conductivity by introducing carrier electrons into the conduction band. This occurs even at room temperature and gives undoped layers fairly low resistivity :

$$\rho\ (S_nO_2) \approx\ 10^{-2}\ (\Omega.cm).$$

The introduction of valence element from five column " V " dopant results in the addition one free electron in the lattice. The resistivity of this n-type semiconductor thus created decreases when the concentration of carriers (electrons) increases.

It is very interesting to say that the electrical properties of monocrystalline and polycrystalline tin oxide are different (that is mean the conductivity mechanisms are

different). The deposited $SnO_2$ layers have a poly-crystalline structure that has a more complex conduction mechanism.

## III.5.Magnetic properties of $SnO_2$ thin films

Dilute magnetic semiconductors with a high temperature are important in spintronics applications. Several studies have been devoted to studying transparent conducting oxides (TCOs) **[49]**, in contrast , there are few studies about the magnetic properties of doped $SnO_2$, for example, Ni doped $SnO_2$ thin films on sapphire substrates grown by PLD **[50]**, magnetic and optical behaviours of $SnO_2$-X thin films with oxygen vacancies prepared by atomic layer deposition **[51]**, another study presents the structural and magnetic properties of Fe/$SnO_2$/Fe thin films **[52]**, swift heavy ion irradiation induced modifications in structural, microstructural, electrical and magnetic properties of Mn-doped $SnO_2$ thin films have also been studied **[53]**.

## III.6.Different phases of tin oxide

Tin oxide films are amorphous when it deposited at temperatures below 350 °C. It is only at this temperature that the crystallization of these films begins. The thin films of tin oxide produced by the various deposition techniques are generally non-stoichiometric, and they present metastable phases such as SnO and $Sn_3O_4$. The SnO phase appears at the deposition temperature of 400 °C and disappears at the temperature of 500 °C. This phase decomposes into $SnO_2$ and Sn at an annealing temperature of 450 °C. This shows that an annealing of the films at 500 °C is necessary to have a good $SnO_2$ stoichiometry, so the most important tin oxides is SnO and $SnO_2$ which are formed by oxidation between each other. All these explanations are shown in Figure12 :

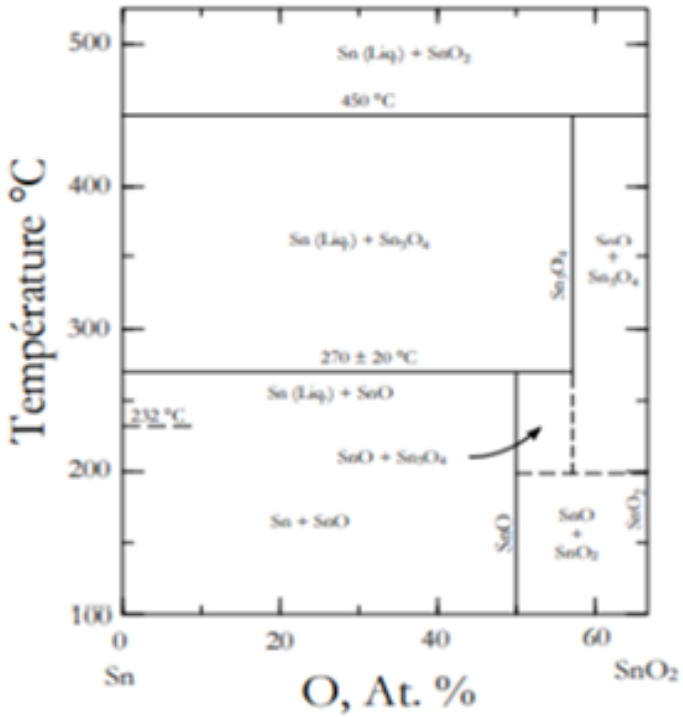


***Figure I.13 :*** *Sn-O phase diagrams for temperatures up to 500 °C* ***[54]****.*

## III.7.Applications of $SnO_2$ thin films

The special electrical and optical properties of $SnO_2$ which makes it unique in comparison with other TCOs and its n-type semiconductor character allow for a large number of applications in various types of fields, the most important of which are:

- Lithium Batteries;
- Solar cells;
- Gas Sensors;
- Electrodes;
- Surface coatings.

-

## IV. Choice of $SnO_2$

The selection of $SnO_2$ in our work is not an accident; its transparency and semiconducting qualities have led us to expect an added value in performance.

This material has already proven itself in solar cells, thermal coatings, and in all of the applications we mentioned at the beginning of this chapter, undoped $SnO_2$ as an antireflection layer can increase the transmission of incident photons and favour the increase of the short-circuit current in the technology of optical window and anti-reflective layer, it can also doped in order to increase its effectiveness in this application (since fluorine-doped tin oxide is a degenerate n-type semiconductor, the ($SnO_2$:F) $N^{++}$/(Si) $N^{+}$ barrier can, by adding to that of the $N^{+}$-P junction, contribute to the increase in open circuit voltage) **[55]**, and also it has increasing attention in the field of catalysis because of its chemical stability **[56]** which is one of the important characteristics of photocatalyst process.

# References

**[01]** K.Mourad, “Elaboration et étude des couches minces d’oxyde d’étain”, University Constantine 1-Algeria, 2018.

**[02]** A. Catellani, A. Calzolari, Codoping and Interstitial Deactivation in the Control of Amphoteric Li Dopant in ZnO for the Realization of p-Type TCOs, Materials. 10 (2017), 332,http://doi.org/10.3390/ma10040332 .

**[03]** Trommer, R.M, "Obtencaocaracterizao de revestimentos de hidroxiapatita sobre substratos de açoinoxidavel 316L utilizando a técnica de deposiçaoquamica de vaporassistidaporchama. Master Thesis", Universidade Federal do Rio Grande do Sul, Brazil (2006 ).

**[04]** W.R. Grove, Phil. Trans. Roy.Soc. London, 142, 87 (1852).

**[05]** Walle, A. J. (2009). Fundamnetals of zinc oxide as a semiconductor. Institute of physics.

**[06]** Peter M. Martin “Handbook of Deposition Technologies for Films and Coatings, Third Edition:Science, Applications and Technology”, Published by Elsevier Inc.2009, ISBN–13: 978-0-8155-2031-3.

**[07]** D. Wang, Fabrication and Characterization of ZnO Related Materials Thin Films for Optical Device Application, doctoral thesis, University of Technology Kochi Japan, 2012

**[08]** Sputtering Sources, Matthew M. Waite, West Chester University of Pennsylvania, West Chester,Pennsylvania; S. Ismat Shah, University of Delaware, Newark, Delaware;David A. Glocker, Isoflux Incorporated, Rochester, New York

**[09]** Pierson, H. O. (1999). Handbook of Chemical Vapor Deposition. New York: Noyes Publication. Q. A. Drmosh, S. (n.d.)

**[10]** D. Perednis and L. J. Gauckler, “Thin Film Deposition Using Spray Pyrolysis,” Electroceramics, vol. 14, pp. 103–111, 2005.

**[11]** L. Madler, "Liquid-Fed Aerosol Reactors for One-Step Synthesis of Nano-Structured Particles," Kona, vol. 22, pp. 107–20, 2004.

**[12]** H. A. Hamedani, "Investigation of Deposition Parameters in Ultrasonic Spray Pyrolysis For Fabrication Of Solid Oxide Fuel Cell Cathodes," Georgia Institute Of Technology, 2008.

**[13]** S. Kaneko, "Spray Pyrolysis Deposition for Thin Film Formation and Its Application to DSC Study," in 24th EU PVSEC, Hamburug, 2009, pp. 432–8003.

**[14]** C. J. Humphreysa, "The significance of Bragg's law in electron diffraction and microscopy, and Bragg's second law," ActaCrystallogr. Sect. A, vol. 69, no. 1, pp. 45–50 2013

**[15]** Y. C. M. Caglar, "The Determination Of The Thickness And Optical Constants Of The Zno Crystalline Thin Film By Using Envelope Method," Optoelectron. Adv. Mater., vol. 8, no. 4, pp. 1410–1413, 2006.

**[16]** D. A. Skoog, Principles of Instrumental Analysis (6 th Ed.). CA : Thomson Brooks/Cole, 2007.

**[17]** E. R. Shaaban, I. S. Yahia, and E. G. El-Metwally, "Validity of swanepoel's method for calculating the optical constants of thick films," Acta Phys. Pol. A, vol. 121, no. 3, pp. 628–635, 2012 .

**[18]** P. K. Manoj, B. Joseph, V. K. Vaidyan, and D. S. D. Amma, "Preparation and characterization of indium-doped tin oxide thin films," Ceram. Int., vol. 33, no. 2, pp. 273–278, 2007 .

**[19]** A. Abdelkrim, S. Rahmane, O. Abdelouahab, A. Hafida, and K. Nabila, "Optoelectronic properties of SnO 2 thin films sprayed at different deposition times," Chinese Phys. B, vol. 25, no. 4, p. 46801, 2016 .

**[20]** D. B. M. Hoffman., S, Martin; W. Choi, "Environmental Applications of Semiconductor Photo Catalysis," Chem. Rev., vol. 95, no. 1, pp. 69–96, 1995 .

**[21]** S. J. Ikhmayies and R. N. Ahmad-Bitar, "A study of the optical bandgap energy and Urbach tail of spray-deposited CdS:In thin films," J. Mater. Res. Technol., vol. 2, no. 3, pp. 221–227, Jul. 2013 .

**[22]** VAN DER PAUW, Philips Research Reports, 13 (1958) 1.

**[23]** R.GREEN, Keithley Instruments, Inc., Keithley Instruments, Inc. (2011).

**[24]** Schematic illustrations of (a) resistivity and (b) Hall effect measurements by the van der Pauw method.

**[25]** L. Hu, R. H. Wei, X. W. Tang, W. J. Lu, X. B. Zhu, Y. P. Sun, Design strategy for p-type transparent conducting oxides Design strategy for p-type transparent conducting oxides, J. Appl. Phys. 128 (2020), 140902, http://doi.org/10.1063/5.0023656.

**[26]** L. Hu, R. H. Wei, X. W. Tang, W. J. Lu, X. B. Zhu, Y. P. Sun, Design strategy for p-type transparent conducting oxides Design strategy for p-type transparent conducting oxides, J. Appl. Phys. 128 (2020), 140902,http://doi.org/10.1063/5.0023656.

**[27]** M. F. Hossain, M. A. H. Shah, M. A. Islam, M. S. Hossain, Transparent conducting SnO2 thin films synthesized by nebulized spray pyrolysis technique: Impact of Sb doping on the different physical properties, Mater. Sci. Semicond. Process. 121 (2021), 105346, http://doi.org/10.1016/j.mssp.2020.105346.

**[28]** A. Abdel-Galil, M. S.A. Hussien, I.S. Yahia, Low cost preparation technique for conductive and transparent Sb doped SnO2 nanocrystalline thin films for solar cell applications, Superlattices and Microstruct. 147 (2020), 106697, http://doi.org/10.1016/j.spmi.2020.106697.

**[29]** W. Allag, H. Guessas, M. Hemissi, M. Boudissa, Study of Erbium Doping Effect on Structural , Morphological and Optical Properties of Dip Coated ZnO Under Alkaline Conditions, Optik. 219 (2020), 165287, http://doi.org/10.1016/j.ijleo.2020.165287.

**[30]** H. Attouche, S. Rahmane, S. Hettal, N. Kouidri, Precursor nature and molarities effect on the optical, structural, morphological, and electrical properties of TiO2 thin films deposited by spray pyrolysis, Optic. 203 (2020), 163985, http://doi.org/10.1016/j.ijleo.2019.163985.

**[31]** H. Nadjette, "Elaboration et caractérisation des couches minces d'oxyde d'indium dopées à l'étain et au brome obtenue par spray pyrolyse ultrasonique", University of Biskra- Algeria, 2021.

**[32]** A. Abdlekrim, "Optimisation des conditions d'élaboration des couches minces d'oxyded'étain SnO2 par spray", University of Biskra-Algeria, 2016.

**[33]** O.R. Alobaidi, P. Chelvanathan, B. Bais, K. Sopian, M.A. Alghoul, M. Akhtaruzzaman, N. Amin, Vacuum annealed Ga:ZnO (GZO) thin films for solar cell integrated transparent antenna application, Mater. Lett. 304 (2021), 130551,http://doi.org/10.1016/j.matlet.2021.130551.

**[34]** X. L. Huang, D.W. Ao, T. B. Chen, Y. X. Chen, F. Li, S. Chen, G. X. Liang, X. H. Zhang, Z. H. Zheng, P.Fan, High-performance copper selenide thermoelectric thin films for flexible thermoelectric application, Mater. Today Energy. 21 (2021), 100743,http://doi.org/10.1016/j.mtener.2021.100743.

**[35]** T. Harada, Thin-film growth and application prospects of metallic delafossites, Mater. Today Adv. 11 (2021), 100146, http://doi.org/10.1.16/j.matdv.2021.100146.

**[36]** S. Yahiaoui, "L'effet de la molarité des différentes sources d'étain sur les propriétés des couches minces d'oxyde d'étain SnO2 élaborées par Spray Ultrasonique", University of Biskra-ALgeria, 2014.

**[37]** WaelHamd, « Elaboration par voie Sol-gel et étude microstructural de gels, de couches minces de SnO2 », 2009.

**[39]** T. Triquet, "Procédé hybride couplant adsorption et photocatalyse pour le traitement de l'eau: élimination de la ciprofloxacine par des fibres de charbon actif fonctionnalisées avec du TiO2", University of Toulouse-Paris, 2021.

**[40 ]** F. Hellegouarc'h "Procédé plasma CVD de dépôt de couches minces d'oxyde d'étain pour l'élaboration de capteurs chimiques" Thèse de doctorat de l'Université Pierre et Marie Curie, 1998.

**[41]** S. Shirakata, A. Yokoyama, S. Isomura «Preparation of SnO2 thin films by plasma-assisted metalorganic chemical vapor deposition " Japanese Journal of Applied Physics, vol35, part2, N°6A, p.722, 1996.

**[42]** L. A. Soares, C. Morais, T. W. Napporn, K. B. Kokoh, P. Olivi, Beneficial effects of rhodium and tin oxide on carbon supported platinum catalysts for ethanol electrooxidation, Journal of Power Sources, 315 (2016), 47-55, http://doi.org/10.1016/j.jpowsour.2016.03.013.

**[43]** R. Sha, S. Badhulika, Facile synthesis of three-dimensional platinum nanoflowers on reduced graphene oxide – Tin oxide composite : An ultra-high performance catalyst for methanol electro-oxidation, J. Electroanal. Chem. 820 (2018) 9-7, http://doi.org.10.1016/j.jelechem.2018.04.057.

**[44]** M. T. Uddin, "Metal oxide heterostructures for efficient photocatalysts", UNIVERSITY OF Darmstadt-Germany, 2013.

**[45]** R. Zair, "Etude et Realisation d'une Cellule Photovoltaique a Heterostructure avec Contact Serigraphie", University of Boumerdes-Algeria, 2007.

**[46]** S. Roguai, A. Djelloul, Elaboration, characterization and applications of SnO2, 2 % Gd- SnO2 and 2 % Gd-9 % F-SnO2 thin films for the photocatalytic degradation of MB by USP method, Inorg. Chem. Commun. 138 (2022), 109308,http://doi.org/10.1016/j.inoche.2022.109308

**[47]** M. Sellami, N. Nguyen, A. Bekka, N. Bettahar, Synthèse et étude des propriétés çmagnétiques avec M = Ca et Pb, Comptes Rendus Chim. 9 (2006), 1209-1214,http://doi.org/10.1016/j.crci.2006.02.001

**[48]** P.C. Preethi, A. Harisankar, U.S. S. Mol, R. Raghunandan, Synthesis of oxydiacetate functionalized strontium coordination polymer through gel diffusion technique: A new dual luminescent chemosensor for the detection of Copper(II) ions and Cr(VI) oxyanions in aqueous medium, Polyhedron. 223 (2022), 115974,http://doi.org/10.1016/j.poly.2022.115974.

**[49]** M. A. A. Masud, M. A. H. Chowdhury, "Analysing the effect of annealing temperature on the crystalline parameters of ZnO nanoparticles", University of Chittagong- Bangladesh, 2019.

**[50]** A. Abdelkrim, S. Rahmane, O. Abdelouahab, N. Abdelmalek, G. Brahim, Effect of solution concentration on the structural, optical and electrical properties of SnO2 thin films prepared by spray pyrolysis, Optik.127 (2016), 2653–2658, https://doi.org/10.1016/j.ijleo.2015.11.232.

**[51]** A. A .Galil, M. S.A. Hussien, I.S. Yahia, Low cost preparation technique for conductive and transparent Sb doped SnO2 nanocrystalline thin films for solar cell applications, SuperlatticesMicrostruct. 147 (2020), 106697,http://doi.org/ 10.1016/j.spmi.2020.106697

**[52]** P. Sivakumar, H. Sharma Akkera, T. R. K. Reddy, Y. Bitla, V. Ganesh, P. M. Kumar, G. S. Reddy, M. Poloju, Effect of Ti doping on structural , optical and electrical properties of SnO2 transparent conducting thin films deposited by sol-gel spin coating, Opt. Mater. 113 (2021), 110845, http://doi.org/10.1016/j.optmat.2021.110845.

**[53]** P.V. Jithin, K. Sudheendran, K.J. Sankaran, J. Kurian, Influence of Fe-doping on the structural and photoluminescence properties and on the band-gap narrowing of SnO2 nanoparticles, Opt. Mater. 120 (2021), 111367, http://doi.org/ 10.1016/j.optmat.2021.111367.

**[54]** Z. Bencharef, A. Chala, R. Messemeche, Y. Benkhetta, The physical properties of spinel cubic Co3O4 thin films prepared by a PSM, Main Gr. Chem. 21 (2022), 329-340, http://doi.org/ 10.3233/MGC-210090.

**[55]** H. Nadjette, "Elaboration et caractérisation des couches minces d'oxyde d'indium dopées à l'étain et au brome obtenue par spray pyrolyse ultrasonique", University of Biskra- Algeria, 2021.

**[56]** Y. Murat, "Nouvelles structures électroluminescentes organiques pour applications signalétiques et petits afficheurs", University of Bordeaux-United State, 2017.

# CHAPTER II

***Tin Oxide thin films Elaboration***

This chapter is presented the experimental procedure beginning with an overview of the spray pyrolysis technique and the reasons for choosing it to deposit $SnO_2$ thin films. The Holmarc apparatus used in the process is described, along with the preparation of precursor solutions, including the chemical reagents and conditions applied. The chapter also introduces the characterization techniques and analytical equipment used to study the structural, optical, and electrical properties of the films.

# I. Spray Pyrolysis Technique

## I.1.Choice of spray pyrolysis technique

Spray pyrolysis is a relatively very simple technique and it uses inexpensive means, It allows to obtain thin or thick films, even multilayered films can be easily prepared with it, however it can used to deposit a wide choice of materials especially transparent conducting oxides (TCOs).

This technique can be classify into several types based on the type of energy source for the precursor reaction , the most important of them are: ultrasonic spray technique (UST) which is based on an ultrasonic wave generator atomizes the solution, and pneumatic spray technique (PST) is depends to a relatively pressurized air flow carry the solution that contains precursors, each one of these techniques can be categorized into four different procedures depending on the temperature (Figure..1):

**Process 1:** the droplet reaches on the substrate; the solvent evaporates leaving a precipitate, which then decomposes, in the solid state.

**Process 2:** the solvent evaporates before the droplet reaches the surface to be coated and the precipitate hits the substrate, decomposing into the solid phase.

**Process 3:** the solvent evaporates, the precipitate melts and vaporizes (or sublimes). There is then diffusion of the vapours towards the substrate and production of a reaction in a heterogeneous phase during contact. This is the classic chemical vapor deposition process. We can notice that it is then possible to define, as in CVD, an evaporation zone and a reaction

zone, the evaporation zone presenting, here, a more complex profile, since the solvent must be evaporated .

**Process 4:** at higher temperature, the chemical reaction no longer takes place in a heterogeneous phase, but in a homogeneous (gaseous) phase with the production of fine powder particles, which can be deposited on the substrate.

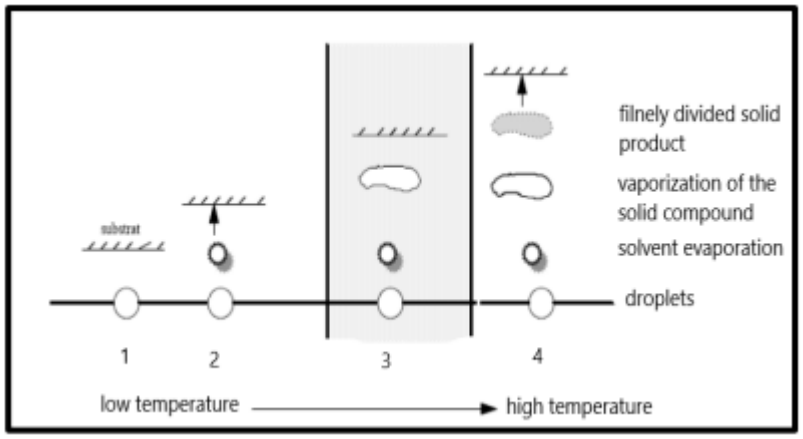


***Figure II.1 :*** *Diagram of decomposition of an aerosol as a function of temperature .* ***[01]***

## I.2. Spray Pyrolysis Equipment (Model : HO-TH-04)

The Holmarc spray pyrolysis system has been specifically designed to meet the requirements of scientific research in the field of thin films, particularly for applications in solar cell development.

In this study, the system was employed at the laboratory of Setif 1 University – Ferhat Abbas, to conduct experiments and achieve the defined research objectives.
This system is distinguished by its ability to automate several complex and error-prone processes that would otherwise be performed manually, thereby ensuring greater accuracy and consistency in results.

Additionally, the ergonomically engineered chamber provides a clean and safe environment that complies with the standards and requirements of modern laboratories.

Parameterslike dispensing rate of the solution and speed of spray head movement which are difficult to control manually are controlled precisely by PC based automation. A positive

displacement pump controlled by stepper motor and microprocessor is used to dispense solution as per requirement. The spray head movement is also controlled by stepper motor driven linear stages in X and Y direction. The temperature of the substrate heater plate is controlled independently through a dedicated controller.**[02]**

***Figure II-1 :****Spray Pyrolysis Equipment(Model : HO-TH-04)****[02]***

## I.2.1.Factors affecting bonding & subsequent build up of the coating

The bonding of the coating to the substrate and the successive build-up of its layers are influenced by several key factors that must be carefully controlled to ensure coating quality and durability. These factors include surface characteristics, processing conditions, and the physical and chemical behavior of the materials during the deposition process. The main factors affecting bonding and subsequent build-up of the coating are as follows:

- Cleanliness
- Surface area
- Surface topography or profile
- Temperature (thermal energy)
- Speed

- Time (reaction rates, cooling rates etc.)
- Physical &chemical properties
- Physical &chemical reactions

A desktop computer with windows OS is used to control the operations through serial port. Our dedicated software for spray pyrolysis system can as well be used for documenting the relevant parameters used for sample preparation like temperature, air pressure, duration, etc.

Spray pyrolysis is a process in which a thin film is deposited by spraying a solution on a heated surface, where the constituents react to form a chemical compound. The chemical reactants are selected such that the products other than the desired compound are volatile at the temperature of deposition. The process is particularly useful for the deposition of oxides and has long been a production method for applying a transparent electrical conductor of Tin oxide ($SnO_2$) or Stannic oxide to glass.

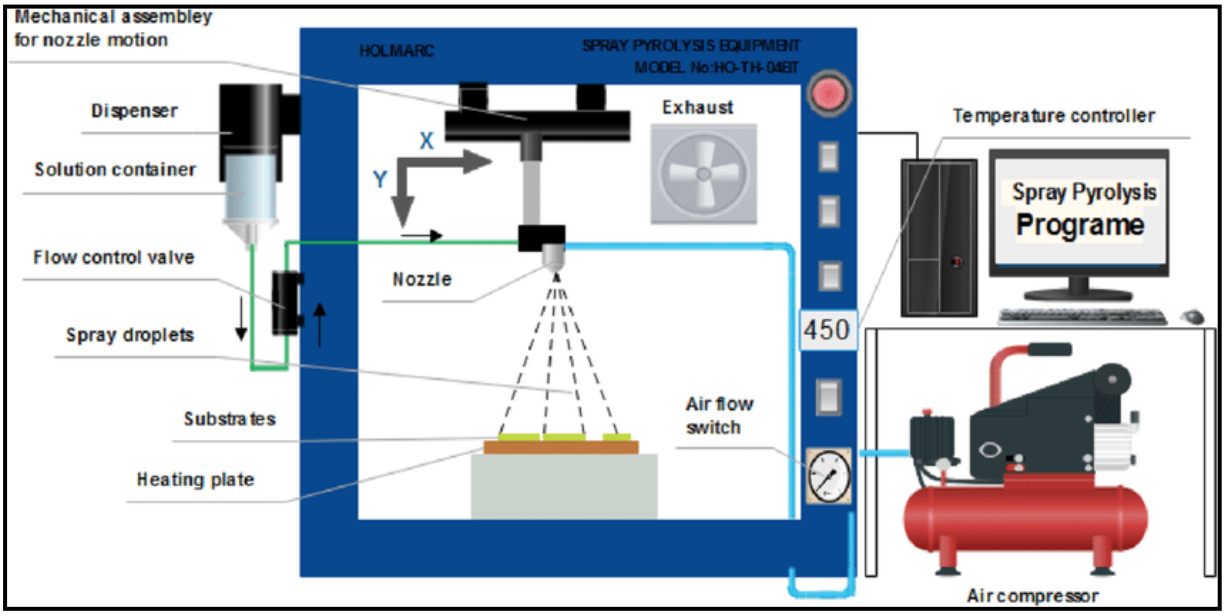


***Figure II.2 :****Spray Pyrolysis Technique****[03]***

## I.2.2. Main Components of the Device

The spray pyrolysis system consists of several key components that work together to ensure accurate, efficient, and uniform thin-film deposition. Each part plays a specific role in the process, as described below:

- ✓ **Solution Container:** Used to hold the chemical solution containing the active material (such as $SnO_2$).
- ✓ **Flow Control Valve:**Regulates the amount of solution flowing out of the container.
- ✓ **Dispenser and Nozzle:** Converts the solution into a fine spray of droplets.
- ✓ **Mechanical Assembly for Nozzle Motion:** Allows the nozzle to move along the X and Y axes to ensure uniform distribution of the spray.
- ✓ **Heating Plate:** Substrates are placed on this plate, which is heated to a specific temperature to facilitate the thermal decomposition of the sprayed solution.
- ✓ **Exhaust Fan:** Removes excess vapors generated during the spraying process.
- ✓ **Air Compressor:** Generates the air pressure required to drive the solution through the nozzle.
- ✓ **Air Flow Switch:** Controls the airflow towards the nozzle.
- ✓ **Temperature Controller and Spray Program:** Manages the surface temperature and controls spraying parameters such as speed, timing, and nozzle movement.

## II.Working Principle

### II.1. Preparation of the Spray Solution

A set of solutions was prepared under controlled conditions. We started by preparing a base solution of tin oxide with molarity **C** equal to 0.05 mol/l.

Which was then doped with zinc and copper—each separately, and both together in a single solution—at a doping concentration of 3% Each one individually.


***Figure II-3 :*** *illustrates the key components employed in this research.*

The doping process was carried out using two different solvents: distilled water and methanol, in order to observe the effect of the solvent type on the resulting thin films.

In total, six solutions were obtained: four prepared with distilled water and two with methanol.

By followingthesesteps:

-Measure a mass of Tin (II) chloride ($SnCl_2$): **m = C.M.V** using a balance (the molar mass M(Sn) = 189,62g/mol and the molar mass of copper M(Cu) = 170.48 g/mol and molar mass of zinc M(Zn) = 219.49 g/mol);


**Figure *II*-4 :** *Measurement of constituent mass via weighing.*

-Preparation of four solutions, the two first one with Zinc incorporation of 3 atm.% concentration and by using of methanol and distilled water as solvents ; the third and fourth solutions were prepared by introducing Copper at 3 atm.% concentration. and dissolved in distilled water and methanol separately.

- Two other solutions have been prepared by a co-doping of (Zn, Cu), at a concentration of 3% for each element, using two different solvents which are: distilled water and methanol.

The previous masses were dissolved separately indistilled water and methanolat a volume

**V = 100ml**;

- The solutions were stirred with ultrasonic bath cleaners for some minutes.
- The six solutions were placed in vials, making them ready for the preparation of thin films preparation.

***Figure II-5 :****Prepared solution.*

## II.2.Substrate Preparation

### II.2.1.Choice of the substrate

The studied films will be deposited onto substrates of solid glass, the choice of glass for reasons:

- Glass is the most commonly selected substrate for all TCO films.
- The good agreement of thermal dilation between glass and $SnO_2$ to minimize the stress
- Interface Film/ Substrate.
- For their transparency that adapts well for the optical characterization of films in the visible.
- For economicreasons.

### II.2.2.Cleaning of the substrates

Cleaning of the Glass substrates is in order to eliminate the traces from greases and impurities onto the surface of glass then ameliorate the film adhesion.

The process of cleaning the surface substrates in all my studies is as follows :

- Firstly we use a pen with diamond point to cut the substrates.
- Rinsing with double distilled water and then with acetone during 10 min.
- Rinsing with double distilled water.

- Washing in methanol at ambient temperature.
- Cleaning in a double distilled water bath drying by using a drier.

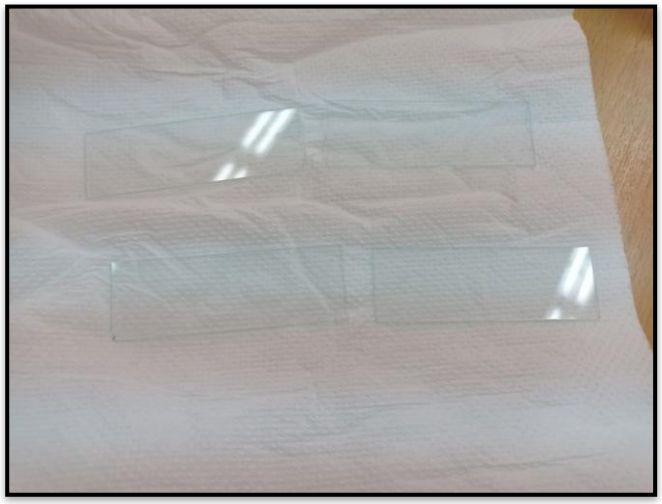

***Figure II-6 :*** *The used Glasses substrates*

## II.2.3.Equipment Settings and Spraying Process

After cleaning the substrates, the solution intended for spraying is placed in a beaker and stirred using a magnetic stirrer for a few minutes. The spraying needle specific to the device is then filled with the solution, with a specific volume for each of the six solutions. Prior to inserting the needle, the device is pre-set to a temperature of **T = 400 °C**. Once the needle is firmly secured and connected to the air compressor from the top, the substrates are placed on the base of the device (the heated plate), which has been previously covered with aluminum foil. After ensuring that all components are properly positioned, the device is activated, and the temperature begins to rise gradually with the start of the process.

The conditions of this process are summarized in the table below. Most of the data were obtained from the computer that controls the device and manages the initiation and termination of the process :

***Table II-1 :*** *Parameters used during the spray operations.*

| No. | Command | Value | Notes |
|---|---|---|---|
| **1** | Home XY | — | Return the nozzle head to the origin point on the X and Y axes |
| **2** | Move | [15, 15] | Move the nozzle to coordinates (15, 15) |
| **3** | Speed | [10, 10] | Initial movement speed on X and Y axes |
| **4** | Wait | 2000 ms | Wait for 2000 milliseconds (2 seconds) |
| **5** | Speed | [5, 3] | Adjust speed to 5 (X-axis) and 3 (Y-axis) |
| **6** | Move | [110 <>, 110 <>] | Back-and-forth motion up to 110 mm on both axes |
| **7** | Air On | — | Activatecompressed air |
| **8** | Spray On | — | Start spraying |
| **9** | Duration | 16 min | Total spraying duration |
| **10** | Flow Rate | 20 µL/min | Liquid flow rate |
| **11** | Flow Factor | 1 | Flow factor set to 1 |
| **12** | Substrates | 7.7 Cm ×2.5 Cm | — |

### II.2.4.Post-Deposition

After completing the spray process, the samples were allowed to cool gradually inside the chamber.

The substrates were then collected for further analysis of the film's structural, optical, and morphological properties using techniques such as XRD, SEM, and UV-Vis spectroscopy.

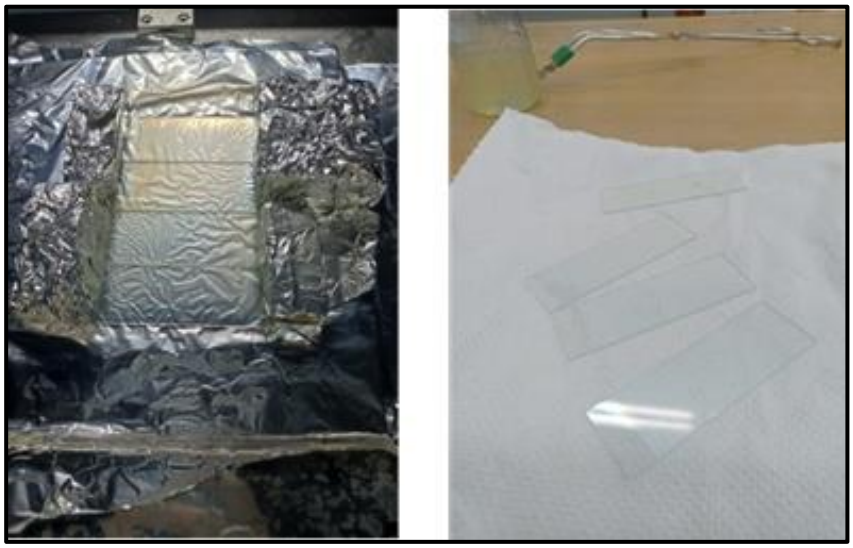

***Figure II-8 :*** *Obtained $SnO_2$ thin films by spray pyrolysis method .*

The obtained samples were named as given in the following table:

**TableII.2:**$SnO_2$ obtained thinfilms.

| Solvent / Dopant (%) | Distilled water | Methanol |
|---|---|---|
| Zn (3%) | ZS1 | ZS2 |
| Cu (3%) | CS1 | CS2 |
| Zn-Cu (3%) | ZC1 | ZC2 |

## II. Characterization techniques

The elaborated films were characterized in order to study their properties.

### III.1. Structural characterisation

XRD measurements were carried out at the Laboratory of Materials Physicochemistry (El-Tarf University), using a Bruker D8 Advance diffractometer, Fig. II-9, in the Bragg-Brentano (θ-2θ) geometry with an angular step of 2θ = 0.02°, using Cu-Kα radiation with a wave length of $\lambda_{Cu}$ = 0.15406 nm.

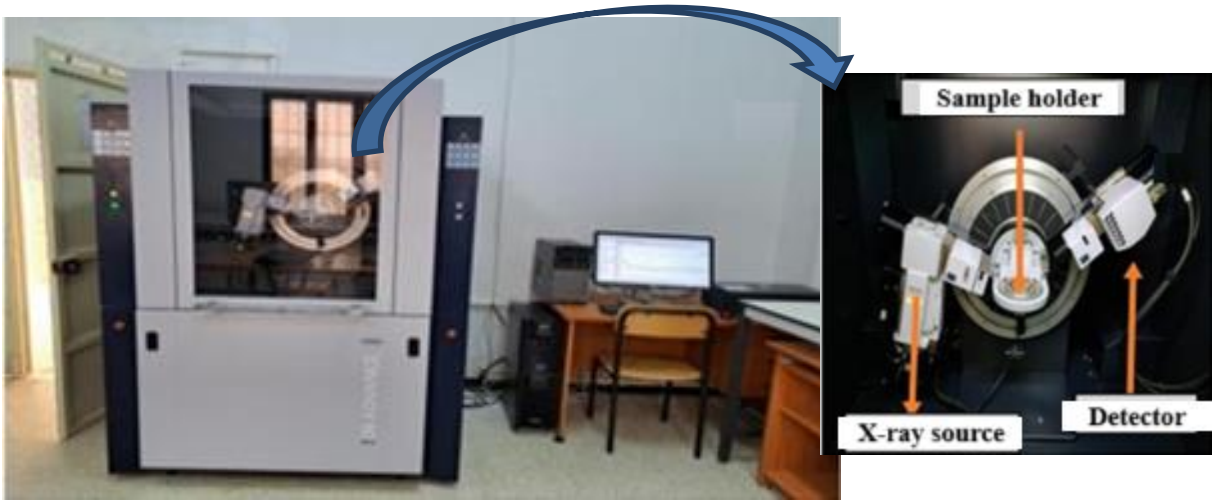


***Figure II-9 :****The used X-Ray diffractometer*.

## III.2. Optical characterization

The optical transmittance, reflectance and absorbance spectra in UV–Visible range were achieved using Perkink Elmer spectrophotometer in the Research Unit in Mining and Metallurgy of Annaba.

***Figure II-10 :****Perkin Elmer Spectrophotometer*.

## III.3. Electrical characterization

The electrical properties were studied via Hall effect method, by using HMS 3000 equipment of Semiconductor laboratory.


***Figure II-10 :****Hall Effect Equipment.*

# References

**[01]** R. Saâd, “Elaboration et caracterisation de couches minces par spray pyrolyse et pulverisation magnetron”, University of Biskra- Algeria, 2008.

**[02]** http://www.holmarc.com/

**[03]** Patil, P. S. "Versatility of chemical spray pyrolysis technique." *Materials Chemistry and Physics*, vol. 59, no. 3, 1999, pp. 185–198.

**[04]** Al-ezzi A.S, Ansari M.N.M. , Photovoltaic Solar Cells : A Review. Applied system innoavation. 2022.

**[05]** https://encyclopedia.pub/entry/26456 (accessed 10 May 2023).

**[06]** Obaideen K, Olabi A.G, Al Swailmeen Y, et al. , Solar Energy: Applications, Trends Analysis, Bibliometric Analysis and Research Contribution to Sustainable Development Goals (SDGs). Sustainability 2023.

**[07]** Beriala M.M, Khemis A.R. , Optimization by simulation of a thin film solar cell based on lead sulphide ( PbS ). Master degree Univeristy of Kasdi Merbah Ouargla 2022.

**[08]** Paulson P, Dutta V, Technology M, Dutta V. Thin-Film Solar Cells: An Overview. Prog. photovolat : Res.Appl . 2004

**[09]** Akhtaruzzaman Md, Selvanthan V, Comprehensive guide on orgainc and inorgainc solar cells. Elsiver.

**[10]** Hossain MK, Toki GFI, Kuddus A, et al. An extensive study on multiple ETL and HTL layers to design and simulation of high-performance lead-free CsSnCl3-based perovskite solar cells. Sci Rep 2023. Chapter 1 Generalities about solar cells 27

**[11]** Hmaitiche A, Djouber S.E . Study and numerical simulation of photovoltaic cells based on chalcostibite materials.Master degree univeristy of Mohammed Boudiaf Msila. 2022.

**[12]** ديبونة عبد الباسط، قماري عبد هللا. محاكاة خلية شمسية باستعمال برنامج سيلفاكو-أطلس. مذكرة ماستر جامعة قاصدي مرباح ورقلة 2022.

**[13]** Ammari M, Dris MH. Theoretical study on perovskite solar cells (Pscs) and their applications. Master degree university of Kasdi Merbah Ouargla 2022.

**[14]** P. A. Basore, "Numerical modeling of textured silicon solar cells using PC-1D," IEEE Transactions on electron devices, vol. 37, pp. 337-343, 1990.

**[15]** J. G. Fossum, "Computer-aided numerical analysis of silicon solar cells," Solid-State Electronics, vol. 19, pp. 269-277, 1976.

**[16]** R. Wei, "Modelling of perovskite solar cells," Queensland University of Technology, 2018.

**[17]** J. Cai and L. Han, "Theoretical investigation on interfacial-potential-limited diffusion and recombination in dye-sensitized solar cells," The Journal of Physical Chemistry C, vol. 115, pp. 17154-17162, 2011.

**[18]** J. Villanueva, J. A. Anta, E. Guillén, and G. Oskam, "Numerical simulation of the current− voltage curve in dye-sensitized solar cells," The Journal of Physical Chemistry C, vol. 113, pp. 19722-19731, 2009.

**[19]** K. Ogiya, C. Lv, A. Suzuki, R. Sahnoun, M. Koyama, H. Tsuboi, N. Hatakeyama, A. Endou, H. Takaba, and M. Kubo, "Development of multiscale simulator for dye-sensitized TiO2 nanoporous electrode based on quantum chemical calculation," Japanese Journal of Applied Physics, vol. 47, p. 3010, 2008.

**[20]** M. Burgelman, P. Nollet, and S. Degrave, "Modelling polycrystalline semiconductor solar cells," Thin Solid Films, vol. 361, pp. 527-532, 2000.

**[21]** A. Niemegeers, S. Gillis, and M. Burgelman, "A user program for realistic simulation of polycrystalline heterojunction solar cells: SCAPS-1D," in Proceedings of the 2nd World Conference on Photovoltaic Energy Conversion, JRC, European Commission, juli, 1998, pp. 672-675.

**[22]** M. Burgelman and J. Marlein, "Analysis of graded band gap solar cells with SCAPS," in Proceedings of the 23rd European Photovoltaic Solar Energy Conference, Valencia, 2008, pp. 2151-2155. Chapter II Numerical simulation by SCAPS 55

**[23]** S. Utilisateur. (2019). Simulation programme SCAPS-1D for thin film solar cells.

**[24]** M. Mostefaoui, H. Mazari, S. Khelifi, A. Bouraiou, and R. Dabou, "Simulation of high efficiency CIGS solar cells with SCAPS-1D software," Energy Procedia, vol. 74, pp. 736- 744, 2015.

**[25]** R. E. Brandt, "Elucidating efficiency losses in cuprous oxide ($Cu_2O$) photovoltaics and identifying strategies for efficiency improvement," Massachusetts Institute of Technology, 2013.

**[26]** D. Korfiatis, S. Potamianou, E. Tsagarakis, and K. T. Thoma, "Demixing profiles in oxides upon the application of an electrical field," Solid state ionics, vol. 136, pp. 1367-1371, 2000.

**[27]** S. P. Gaur and D. H. Navon, "Two-dimensional carrier flow in a transistor structure under nonisothermal conditions," IEEE Transactions on Electron Devices, vol. 23, pp. 50-57, 1976.

**[28]** H. Mathieu and H. Fanet, Physique des semiconducteurs et des composants électriques: cours et exercices corrigés: Dunod, 2009.

**[29]** M. Burgelman, K. Decock, A. Niemegeers, J. Verschraegen, and S. Degrave, "SCAPS manual," ed: February, 2016.

**[30]** H. Pauwels and G. Vanhoutte, "The influence of interface state and energy barriers on the efficiency of heterojunction solar cells," Journal of Physics D: Applied Physics, vol. 11, p. 649, 1978.

# CHAPTER III

***Results and Discussion***

# Introduction

As commonly known, $SnO_2$ thin films properties are significant effected bytechnique of elaboration and deposition parameters. The purpose of this chapter is to present and interpret the experimental results of this work which aims the elaboration and characterization of tin sulphide thin films deposited on glass substrates by spray pyrolysis technique at different solvent and doping.

## III.1. Structural properties

### III.1.1. XRD analysis

X-ray diffraction (XRD) analysis was performed to evaluate the crystalline quality of both undoped and doped $SnO_2$ thin films deposited at a substrate temperature of 400 °C. The corresponding XRD patterns are presented in Figures III.1 and III.2. All major diffraction peaks were identified based on standard JCPDS data (Card No. 029-1484).

Figure III.1 illustrates the diffraction patterns of $SnO_2$ films synthesized using distilled water as a solvent, with Zn and Cu employed as dopants.

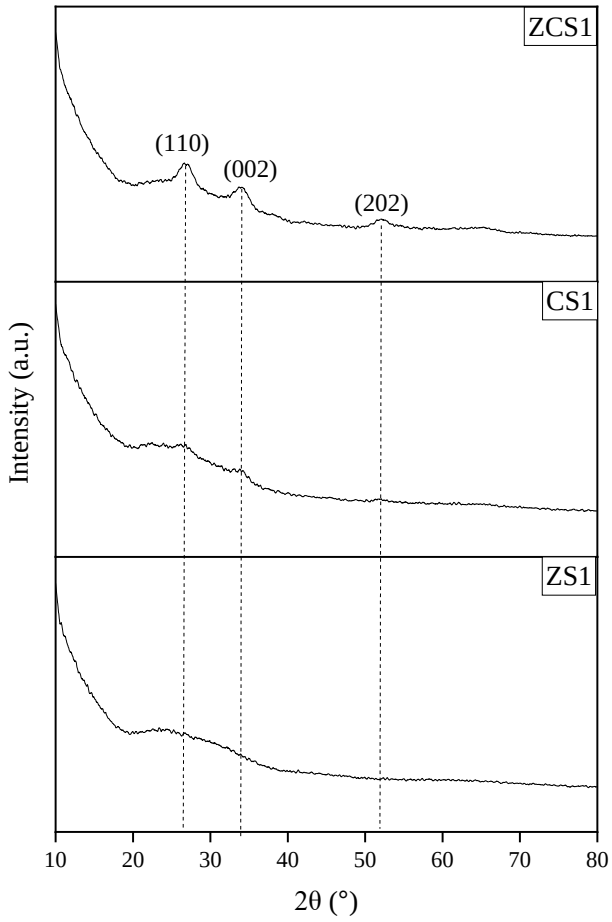


**FigureIII.1.***XRD patterns of tin sulfide as function of Zn and Cu doping.*

Figure III.1. confirms that the all deposited (ZS1, CS1, ZCS1) using distilled water as a solvent and with a fixed dopant concentration of 3 at.% maintain the tetragonal rutilestructure of $SnO_2$. The labeled peaks (110), (002), and (202) match the reference.These peaks are clearly observed in the ZCS1 sample, slightly less in CS1, and significantly broadened and less intense in ZS1, indicating differences in crystallinity and possibly crystallite size.Further more, we notice the absence of secondary phases, where no extra peaks are visible within the shown 2θ range (10°-80°). This indicates:

- The effective doping of $Zn^{2+}$, $Cu^{2+}/Cu^{+}$, and both are successfully incorporated into the $SnO_2$ lattice as substitutional dopants (replacing $Sn^{4+}$) within their solubility limits at 3 atm.%.**[1]**

- No detectable Oxide formation because no peaks corresponding to ZnO (e.g., ~31.8°, 34.4°, 36.3°), CuO (~35.5°, 38.7°) or $Cu_2O$ (~36.4°) were observed. This suggests the dopants are dissolved atomically**[2]**.

**Zn-doped $SnO_2$ (ZS1):** The XRD pattern shows a broad halo with very weak or poorly defined peaks, especially around (110) and (002). This is can be due to the fact that $Zn^{2+}$ has an ionic radius (~0.74 Å) close to that of $Sn^{4+}$ (~0.69 Å), so it can substitute Sn in the lattice, but high Zn content or poor solubility in water may disrupt the growth of a well-ordered crystal structure**[3-5]**.

**Cu-doped $SnO_2$ (CS1):**XRD shows slightly more defined peaks compared to ZS1, but still broad and of low intensity.This indicates a moderate crystallinity, which can be explained by $Cu^{2+}$ ions (~0.73 Å) can also substitute $Sn^{4+}$, but might introduce more oxygen vacancies and lattice distortion due to the change in oxidation state ($Sn^{4+}$ to $Cu^{2+}$)**[3]**.

**Zn–Cu co-doped $SnO_2$ (ZCS1):**This sample exhibits well-defined peaks corresponding to (110), (002), and (202) planes of tetragonal $SnO_2$with an improved crystallinity. Co-doping might stabilize the lattice through charge compensation between $Zn^{2+}$ and $Cu^{2+}$, balancing defect generation and enhancing crystal growth.

Figure III.2 displays the XRD patterns of $SnO_2$ thin films prepared using methanol as the solvent, in which Zn and Cu were incorporated as dopant elements during the synthesis process.

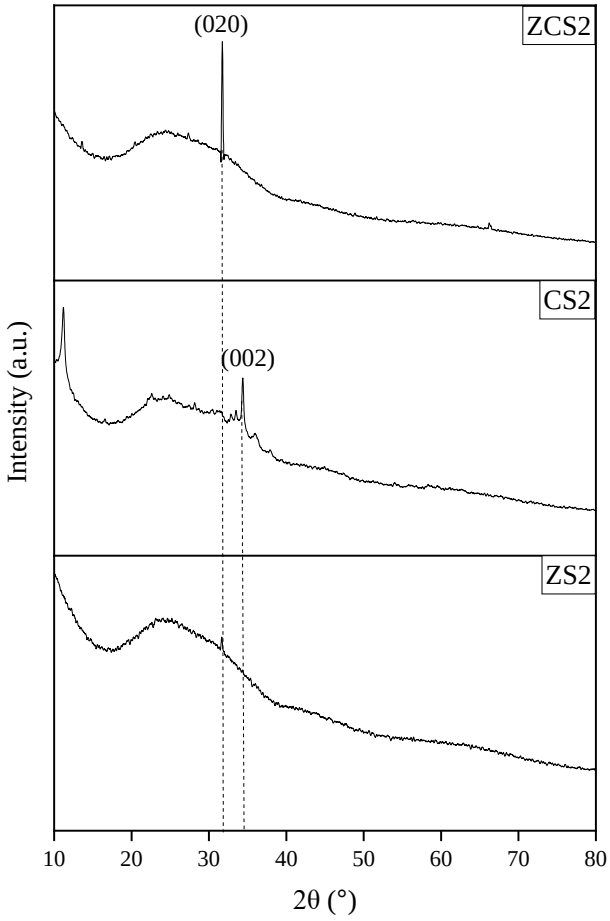


**Figure III.2:***X-ray diffraction patterns of tin sulfide thin films synthesized using methanol as the solvent with Zn and Cu dopants.*

Compared to water, methanol offers higher volatility and lower surface tension**[6]**, which typically enhances precursor reactivity and hydrolysis, and accelerates nucleation and grain growth.This explains the sharper and more defined peaks in CS2 and ZCS2, particularly the exceptional crystallinity in ZCS2.

Conferring to the figures III.1 and III.2 we can interpret the effects of dopant and solvents as:

**A. Dopant Effects:**

- $Zn^{2+}$ likely causes more lattice disorder when used alone, possibly due to mismatch in oxidation state and impact on oxygen vacancies**[7]**.
- $Cu^{2+}$ seems to promote nucleation better, especially in methanol**[8]**.

- Co-doping (Zn-Cu) helps stabilize the structure through charge balance and defect control, enhancing grain growth and orientation.

**B. Solvent Effect :**

Due to its faster evaporation and higher chemical reactivity, Methanol, facilitates the uniform precursor mixing, better nucleation and orientation, and higher crystallinity in doped films.

Solvent type plays a significant role: methanol enables better structure formation, especially in co-doped and Cu-doped systems.

## III.2.Optical properties

The optical absorption, transmission and reflection measurements in the wave length range 350-800nm, which are performed to investigate the effect of different parameters on the optical performance of $SnO_2$ thin layers, are plotted in figures III.3and III.4.

The UV–vis–NIR optical data shows consistent figures of how doping, co-doping, and solvent choice govern film transparency, absorption edge, and scattering.

### A. Absorbance

Figure III.3 shows the effect of the doping, co-doping and solvent effect on the absorption as a function of the wavelength.

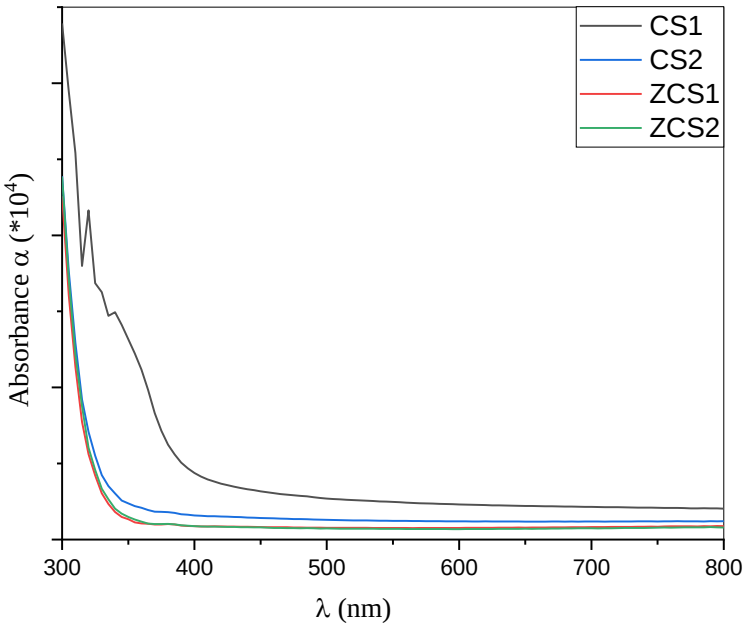


***FigureIII.3:****Absorbance spectra of $SnO_2$ thin films.*

Figure III.3 shows that the film obtained by Cu incorporation CS1 (Cu-water) has by far the highest absorbance across 300–800 nm.Likely, due to its poor crystallinity (small, defective grains) and possibly rougher surface, which increases light trapping and non-radiative scattering.Moving to CS2 (Cu-Methanol), absorbance drops significantly. This behavior can be explained by the fact that methanol gives better crystal quality (as we saw in XRD), fewer defects, and a thinner effective optical path (denser packing), so less parasitic absorption**[9]**.

Furthermore, it can be noticed for the samples ZCS1 (Zn–Cu-water) and ZCS2 (Zn–Cu-Methanol) sit at the bottom of the absorbance scale, with ZCS2 the lowest.Co-doping stabilizes the rutile lattice and reduces sub-bandgap defect states, cutting down on tail absorption in the visible. According to these results, it can be concluded that using Methanol and co-doping synergize to minimize defect-mediated absorption.

## B. Band gap energy (Eg)

To evaluate the band gap energy (Eg) of $SnO_2$ sprayed thin films we have used the Taucformula which indicated that the relation between the energy of incident photon light ($h\upsilon$) and the absorption coefficient ($\alpha$) as following **[10]**:

$(\alpha h\upsilon)^2 = A\,(h\upsilon - Eg)$ III.1

Where α is the absorption coefficient, Eg the energy band gap, A is a constant and hυ is the absorbed photon energy.

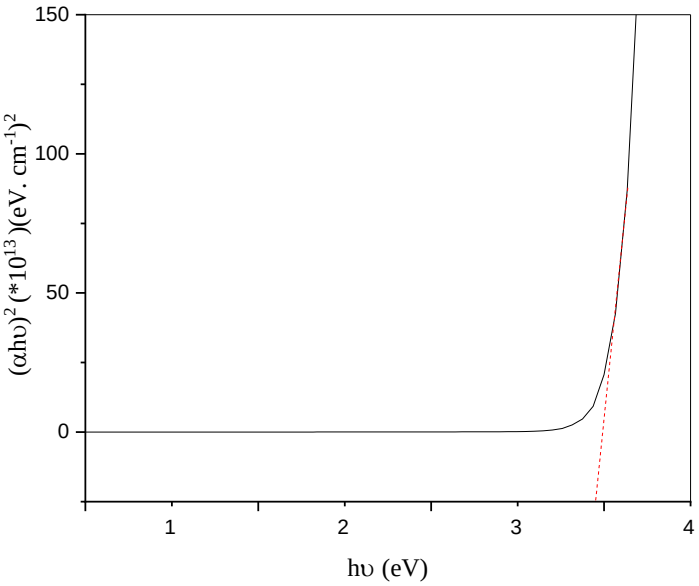


***Figure III.4:*** *Plots of $(\alpha h\upsilon)^2$ versus photon energy (hυ) of CS1 thin film.*

The linear dependence of $(\alpha h\upsilon)^2$ on hυ at higher photon energies indicates that the obtained $SnO_2$ thin films are essentially direct-transition-type semiconductors. Extrapolation of the linear portion of $(\alpha h\upsilon)^2$ to zero gives the value of Eg**[11, 12]**.

The values of Eg for the four samples are given in the table III.1.

**Table III.1:***Eg variation for $SnO_2$ thin films.*

| Sample | Eg (eV) |
|---|---|
| **CS1** | 3.45 |
| **CS2** | 3.55 |
| **ZCS1** | 3.70 |
| **ZCS2** | 3.75 |

According to this table, it can be deduced the Cu incorporation into $SnO_2$ mesh leads to a lower values of Eg, which means a Red-shifts, this later correlate with defect states from $Cu^{2+}$ in a disordered lattice (CS1 and CS2). Nevertheless, by using the co-doping

(ZCS1/ZCS2) the band gap rises significantly and Blue-shifts appear due to crystallinity improvement, or when strain from co-doping enlarges the effective gap.

## C. Transmittance and Reflectance

Figure III.4 (A and B) depicts the variation of the transmittance (T) and the reflectance (R) of the doped and co-doped films obtained by using distilled water and methanol.

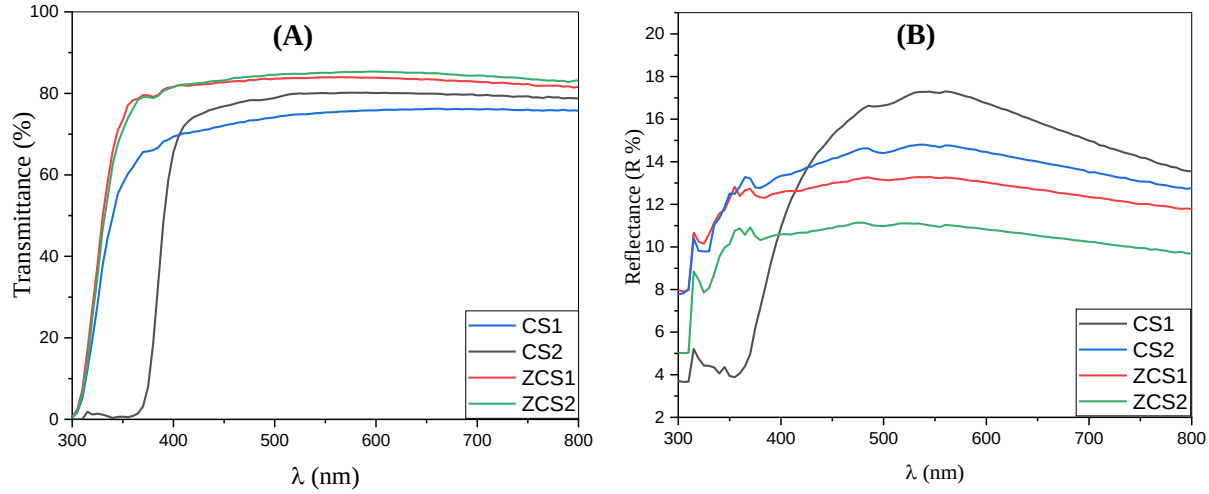


**FigureIII.4:***Transmittance**(A)** and reflectance**(B)**spectraof $SnO_2$thin films.*

According to the figure III.4 (A), it can be noticed that the all four films show a sharp rise in T around λ ≈ 300–350 nm, marking the optical absorption edge of $SnO_2$ (Eg ~3.6–3.8 eV). Additionally, Co-doping boosts transparency by ~20 % over single Cu-doping**[13]**.Also, methanol improves T by ~10 % compared to the distilled water even for the same dopant scheme.

Figure III.4 (B), shows the variation of the reflectance as a function of the wavelength. The sample of $SnO_2$: Cu (water) named CS1, tops the chart with R rising from ~4 % at 300 nm to ~18 % at 600 nm, a sign of high surface roughness and internal scattering. In the other hand the film of $SnO_2$: Cu obtained by using methanol CS2 is lower (~3–15 %), showing methanol-derived films have smoother surfaces and more uniform thickness. Finally, the co-doped films ZCS1(~8–14 %) and ZCS2 (~6–12 %) exhibit the lowest reflectance, confirming the most optically “invisible” films among the four.

## III.3. Electrical properties

The obtained results of the electrical measurements for $SnO_2$ thin films are summarized in Table III.2. All the thin films have negative Hall coefficient, which confirms the n-type electrical conductivity.

**Table III.2:** Resistivity (ρ), Carrier concentration, mobility (μ) and the conductivity type of $SnO_2$ films.

| Sample | ρ (Ω.cm) | Carrier concentration ($x10^{13}$ $cm^{-3}$) | μ ($x10^{2}$ $cm^2.V^{-1}.s^{-1}$) | Conductivity type |
|---|---|---|---|---|
| CS1 | 200.22 | 3.84 | 0.30 | N |
| CS2 | 170.82 | 9.43 | 0.38 | N |
| ZCS1 | 150.21 | 11.67 | 2.08 | N |
| ZCS2 | 110.65 | 11.55 | 4.00 | N |

It can be noticed that all samples remain n-type and the resistivity decrease from ~200 to ~111 Ω.cm. This behavior can be explained by the fact that both higher carrier density and higher mobility push ρ down ward **[14, 15]**.

Moreover, the increasing in the carrier concentration can be justified by: methanol promotes more complete precursor decomposition and creates more oxygenvacancies (each acting as an n-type donor), so Cu-doped films in methanol are roughly twice as doped as those in water. In the other hand, Co-dopingwith Zn adds additional donor states or helps stabilize the $SnO_2$ matrix so more electrons are freed pushing n up further in ZCS1.

# References


**[1]** Abbas, S.I., Lattar, A.M.A., Al-Azawy, A.A., 2023. Enhanced ultraviolet photodetector based on Al-Doped ZnO thin films prepared by spray pyrolysis method. J. Optics. 52 (2).

**[2]** Al Ogaili, H.A.T., Abbas, S.I., Mohammed, M.A., Raman spectra and electronic features for nanotubes of znssewurtziod: Ab-initio, 2020. ChalcogenideLett., 17, 251–255; https://chalcogen.ro/251_OgailiHAT.pdf.

**[3]** Avach, M.L., Difallah, M., Benhaoua, B., 2023. Nonlinear optical properties of cobalt doped SnO2 thin films. Optik 272, 296170. https://doi.org/10.1016/j. ijleo.2022.170296.

**[4]** Batal,M.A., Nashed, G., Jneed, F.H., 2012. Electric properties of Nanostructure Tin Oxide thin film doped with Copper prepared by Sol-Gel Method. Lat Am. J. Phys. Educ. 6, 311–316.

**[5]** M. Dhaouadi, M. Jlassi, I. Sta, I. Ben Miled, G. Mousdis, M. Kompitsas, and W. Dimassi, Physical properties of copper oxide thin films prepared by sol-gel spin – coating method, Am. J. Phys. Appl..6 (2), (2018) 43–50. 10.11648/j.ajpa.20180602.13.

**[6]** El Radaf L. M., Hameed T. A., El Komy G. M., Dahy T. M., 2019. Synthesis, structural, linear and nonlinear optical properties of chromium doped SnO2 thin films, Ceramics Int., 45,3077–3080.

**[7]** El Radaf L. M., Hameed T. A., El Komy G. M., Dahy T. M., 2019. Synthesis, structural, linear and nonlinear optical properties of chromium doped $SnO_2$ thin films, Ceramics Int., 45,3077–3080.

**[8]** Habte, A.G., Hone, F.G., Dejene, F.B., 2022. Influence of Cu –doping concentration on the structural and optical properties of $SnO_2$ nanoparticles by Co-precipitation route. J. Nanomater. 5957125.

**[9]** Islam, A., Mou, J.R., Hossain, F., Hossain, S., 2020. Highly transparent conducting and enhanced near–band edge emission of $SnO_2$: Ba thin films and its structural, linear and nonlinear optical properties. Opt. Mater. 106 (109996).

**[10]** Hadef, Z., Kamli, K., Akkari, A. et al. In-depth characterization of physical proprieties of SnS:Mg thin films fabricated by ultrasonic spray for solar cell applications. J Mater Sci: Mater Electron 35, 1632 (2024).

**[11]** Pan Z, et al. Investigation of optical and electronic properties in Al-Sn co-doped ZnO thin films. Mater SciSemicond Process 2013;16(3):587e92.

**[12]** Basyooni MA, Shaban M, El Sayed AM. Enhanced gas sensing properties of spin-coated Na-doped ZnO nanostructured films. Sci Rep. 2017;7(August 2016):1e12.

**[13]** Strbac, D.D., Lukic-Petrovic, S.R., Petrovic, D.M., Strbac, S.R., Tverhanovich, A., 2015. Effect of Cu variation on the optical and structural properties of thermally deposited Cu-AsSe1.4 I0.2 thin films. ChalcogenideLett. 12 (75–84).

**[14]** Radaf I. M., Hameed T. A., Dahy T. M. and EL-Komy G. M., 2018. Synthesis, structural, linear and Nonlinear optical properties of chromium doped $SnO_2$ thin films. Ceram. Int., 45, 3 10.1016/j.ceramint.2018.10.189.

**[15]** V. Mazumder, Aishani, Chung Kim Nguyen, Thiha Aung, Mei Xian Low, MdAtaur Rahman, et All., Long duration persistent photocurrent in 3 nmthin doped indium oxide for integrated light sensing and in-sensor neuromorphiccomputation, Adv. Funct. Mater. (2023) 2303641.

# CONCLUSION

In this study, tin dioxide ($SnO_2$) thin films were successfully deposited on glass substrates using the spray pyrolysis technique at a substrate temperature of 400 °C. The films were synthesized using different doping elements (Zn, Cu, and their combination) and two types of solvents (distilled water and methanol) in order to investigate their effects on the structural, optical, and electrical properties of the films.

X-ray diffraction analysis revealed that all deposited films retained the tetragonal rutile structure of $SnO_2$, without any secondary phases. The co-doped films, especially those prepared using methanol, showed enhanced crystallinity, indicating a more stable and well-ordered lattice structure due to better dopant incorporation and solvent effects.

Optical measurements demonstrated that doping and solvent type significantly influenced the films' absorbance, transmittance, and energy band gap. The co-doped films exhibited higher transparency and a wider optical band gap, reaching up to 3.75 eV, indicating reduced defect states and improved film quality. Methanol-based films, in particular, displayed lower reflectance and smoother surfaces.

Electrical characterizations confirmed that all films exhibited n-type conductivity. Co-doping with Zn and Cu, especially in methanol, led to the lowest resistivity (\~110 Ω·cm) and highest mobility ($4.00 \times 10^2$ $cm^2/V \cdot s$), due to the combined effects of increased carrier concentration and improved crystal quality.

# CONCLUSION

In conclusion, the spray pyrolysis technique proved to be an effective, low-cost method for producing high-quality $SnO_2$ thin films. The combined use of Zn–Cu co-doping and methanol as a solvent resulted in films with enhanced structural integrity, better optical performance, and improved electrical conductivity, making them excellent candidates for applications in transparent conductive oxides and thin-film solar cells.